Characterization of the ROS Production in Ischemia/Reperfusion-induced Lung Injury

Inaugural Dissertation
submitted to the
Faculty of Medicine
in partial fulfilment of the requirements
for the PhD-Degree
of the Faculties of Veterinary Medicine and Medicine
of the Justus Liebig University Giessen

by

Akylbek Sydykov
of
Osh, Kyrgyz Republic

Giessen 2009

From the Medical Clinic II, University of Giessen Lung Centre

Chairman: Werner Seeger, Prof., M.D.

of the Faculty of Medicine of the Justus Liebig University Giessen

First Supervisor and Committee Member:	Prof. Dr. Ardeschir Ghofrani
Second Supervisor and Committee Member:	Prof. David B. Pearse, MD
Committee Member (Chair):	Prof. Dr. Wolfgang Kummer
Committee Member:	Prof. Dr. Joachim Roth

Date of Doctoral Defence: 27th of October, 2009

Index of contents

Index of tables

Index of figures

1. Introduction

1.1. Pathophysiology of ischemia/reperfusion lung injury

1.1.1. Definitions

Cellular damage caused by restoration of blood supply to previously viable ischemic tissues is defined as ischemia/reperfusion (IR) injury. The consequences of depriving an organ of its blood supply (ischemia) have long been recognized as a critical factor in the clinical outcome of stroke, myocardial infarction and organ transplantation. Although restoration of circulation (reperfusion) is essential for the recovery of normal cellular function and prevention of irreversible tissue injury, reperfusion may itself initiate a series of pathophysiological alterations that can augment tissue injury in excess of that produced by ischemia alone. For example, it was demonstrated in a feline model of intestinal ischemia that 4 h of ischemia alone caused less severe injury than 3 h of ischemia followed by 1 h of reperfusion.[1]

The absence of oxygen and nutrients from blood creates a condition in which the restoration of circulation results in inflammation and oxidative damage through the induction of oxidative stress rather than restoration of normal function. Tissue injury after reperfusion may have serious consequences depending on the organ, e.g., myocardial infarction or stunning, stroke, and injury after organ transplantation or cardiac bypass surgery. In the lung IR injury is characterized by impairment of gas exchange, increased microvascular permeability because of endothelial dysfunction and injury and ensuing pulmonary edema.[2, 3] Lung IR injury can adversely affect graft function in the early post-transplantation period, leading to primary graft failure with increased morbidity and mortality in transplant patients.[4] Despite substantial advances in lung preservation and improvements in surgical techniques and perioperative care IR-induced lung injury remains an important cause of early morbidity and mortality in transplanted patients.[5] In addition to significant morbidity and mortality in the early postoperative period severe IR injury can also be associated with an increased risk of acute rejection that can adversely affect graft function in the long term.[6] IR-induced injury may also occur in a variety of other clinical conditions, including reperfusion after thrombolytic therapy,[7] pulmonary thromboendarterectomy,[8, 9] myocardial infarction,[10] cardiopulmonary bypass surgery,[11, 12] severe circulatory shock,[13] and stroke.[14] Because diseases due to ischemia (e.g., myocardial infarction and stroke) are exceedingly

common causes of morbidity and mortality in the population and because organ transplantation has had increasing success and has become the mainstay of therapy for most end-stage diseases, understanding the pathomechanisms of IR injury has the potential to lead to therapies that could improve public health.

1.1.2. Organ ischemia

Oxygen as a basic fuel is essential to cell function. Interruption of the blood supply to a tissue initiates a sequence of events leading to cellular dysfunction and death. The severity of ischemic injury is determined by both the duration and the extent of blood flow decrease to an organ or tissue.[15] During ischemia, an inadequate supply of O_2 leads to a cessation in adenosine triphosphate (ATP) synthesis and the cell is deprived of the energy needed to maintain homeostasis. Anaerobic metabolism becomes the main source of ATP production. Decreased ATP inactivates the ATP-dependent cell membrane pumps resulting in even greater cellular dysfunction. Inefficient removal of waste products may eventually lead to increased local accumulation of lactic acid. The resulting acidosis alters normal enzyme kinetics. Furthermore, the activation of nuclear factor-kB during ischemia initiates inflammatory reactions. Increased expression of adhesion molecules favours augmented polymorphonuclear leukocytes adhesion at the site of IR injury during reperfusion.

1.1.3. Reperfusion of the ischemic organ

Reperfusion is an absolute prerequisite for cellular salvage and recovery from ischemic injury as re-establishing blood flow leads to restoration of the energy supply and removal of waste products. However, reperfusion itself may lead to additional tissue injury beyond that generated by ischemia alone, thus representing the “double edged sword”.[16] On reperfusion, reintroduction of abundant oxygen at the onset of reperfusion evokes within the first few minutes of reflow a burst of potent reactive oxygen species (ROS). Activation and accumulation of leukocytes in the tissue result in release of ROS, proteases, cytotoxic and chemotactic substances, that further amplify the infiltration of neutrophils. Longer periods of ischemia can lead to physical obstruction of capillaries, the so called no-reflow phenomenon. Cellular edema may also cause capillary plugging during reperfusion thus contributing to this phenomenon. A rise in pulmonary artery pressure is frequently seen after reperfusion, in both lung transplantation recipients[17] and animal models[18-20] This rise in

hydrostatic force may further increase extravascular accumulation of protein in the lung interstitium during reperfusion.

1.1.4. Leukocytes and ischemia/reperfusion

A deleterious role for circulating polymorphonuclear leukocytes in lung IR has been inferred from the protective effect of polymorphonuclear leukocyte depletion[21] and reduced injury following adhesion molecule inhibition,[22-25]. After ischemia, local tissue reperfusion generates a number of inflammatory mediators that attract circulating leukocytes. Cell adhesion molecules on the leukocyte surface bind to ligands on endothelial cells, initiating a sequence of events resulting in extravasation of leukocytes from the microvasculature. Activated neutrophils can cause tissue injury via ROS generation during the respiratory burst.[26] They also release potent proteolytic enzymes capable of degrading almost all components of the endothelial basement membrane as well as junctional proteins that maintain endothelial barrier function.[27] In addition, progressive microcirculatory obstruction by leukocytes in the microcirculation underlying the no-reflow phenomenon may limit adequate perfusion after reperfusion. Thus, a vicious cycle occurs during reperfusion, with continued neutrophil chemotaxis and activation leading to additional ROS formation, endothelial damage, and capillary plugging.

Although many investigations have confirmed the role of neutrophils in reperfusion injury, others have questioned neutrophil involvement. Deeb and colleagues demonstrated that neutrophils are not necessary to induce reperfusion injury in a rat lung preparation using isolated blood cell components.[28] Neutrophil-independent reperfusion injury using anti-rat neutrophil antibodies was also demonstrated in an in vivo rat lung model at 90 minutes of reperfusion.[29] Their study demonstrated that the injury was not associated with polymorphonuclear leukocyte sequestration. Eppinger et al[30] in a similar in vivo study found that during lung IR, there is a bimodal pattern of injury, consisting of both neutrophil-independent and neutrophil-mediated events. These findings suggest neutrophil involvement in reperfusion injury occurs during the late phase of reperfusion and that other cells are responsible for the earliest phase of reperfusion injury. As early injury occurs well before significant tissue neutrophil infiltration has occurred, it is likely dependent on a resident cell type such as the alveolar macrophage. However, the role of resident lung leukocytes in lung IR injury remains controversial.

Pulmonary macrophages consist of different sub-populations, i.e., alveolar macrophages as well as interstitial, pleural, and vascular macrophages.[31] Vascular macrophages exist in the sheep, the calf, and the goat, but not in rodents.[31] Alveolar macrophages comprise the majority of pulmonary resident leukocytes in rodents.[32] Although, alveolar macrophages play a crucial role in the defence system of the lung, they also can induce damage to the lung.[33, 34] Activated macrophages can contribute the pathogenesis of tissue injury by releasing an array of mediators, including proinflammatory and cytotoxic cytokines, bioactive lipids, hydrolytic enzymes, ROS, and nitric oxide. Inhibition of macrophage function with gadolinium chloride [35-37] as well as depletion of alveolar macrophages by clodronate liposomes protects lungs from IR-induced injury.[38, 39] In contrast, Nakamura et al [40] demonstrated that intratracheal administration of liposome-encapsulated clodronate does not benefit, but aggravates, warm ischemia-reperfusion injury of the lung.

1.1.5. Endothelial cells and ischemia/reperfusion

The endothelium is strategically located at the interface between the wall of blood vessels and the blood stream and is "not just a cellophane wrapper".[41] The endothelial lining of blood vessels is an active tissue that plays a pivotal role in maintaining vascular homeostasis. Endothelial cells sense mechanical stimuli, ambient PO_2, and hormonal stimuli and respond with appropriate changes in function to maintain homeostasis. They exert significant autocrine, paracrine and endocrine actions and regulate vasomotor function and tissue perfusion.[42] Endothelial cells also modify the inflammatory processes by regulating the expression of the adhesion molecules that bind to neutrophil integrins and mediate neutrophil infiltration.[43] The endothelium also plays a significant role in the regulation of hemostasis.[43]

The increased generation of ROS during reperfusion after ischemia contributes to tissue injury, microvascular dysfunction, increased endothelial permeability, and endothelial "stunning".[44] Endothelial activation may serve to further enhance ROS production through the recruitment and activation of leukocytes.

1.2. Evaluation of lung injury in isolated lungs

Normal pulmonary function and tissue integrity depend on the maintenance of fluid balance. Lung injury can be applied to conditions ranging from mild interstitial edema without tissue injury to massive and fatal destruction of the lung. Accumulation of pulmonary edema can result either from increased vascular filtration pressure or increased permeability of the pulmonary microvascular endothelial barrier. The methodologies employed for lung injury assessment range from non-specific measurement of edema formation to techniques for calculating values of specific permeability coefficient for the microvascular membrane in pulmonary vessels. Additionally, microscopic techniques can provide qualitative verification of lung injury and/or hydrostatic edema but are less useful for evaluating global lung dysfunction.[45]

1.2.1. Measurement of pulmonary edema

Formation of pulmonary edema can be quantitatively assessed using gravimetric techniques. There are four methods commonly applied in *in vivo* experiments: the lung wet weight, the lung wet weight/body weight ratio, the lung wet/dry weight ratio, and the extravascular lung water.[45] In isolated perfused lung preparations lung weight can be monitored throughout experiment using a strain gauge force transducer. However, quantification of accumulated fluid alone does not allow discrimination between hydrostatic and permeability edema.

1.2.2. Permeability measurements

A variety of techniques for assessment of lung vascular permeability may be applied to isolated perfused lung preparations. Most are based on the extravascular escape of indicated molecules or the measurement of transvascular fluid filtration under conditions of hydrostatic challenge.[46]

The determination of the capillary filtration coefficient (Kfc) is the most commonly used method for quantifying the lung microvascular barrier that has been used in numerous studies in isolated perfused lung preparations. Kfc characterizes the microvascular hydraulic conductivity and can be measured by gravimetric, indicator hemoconcentration, or tracer methods.[47] The gravimetric method involves establishing a sustained step increase of the venous pressure to induce steady gain of lung weight. Gravimetric Kfc is calculated as the ratio of the rate of lung weight gain to the induced pressure increase. Kfc only increases with

lung injury and do not change with time, blood flow, and high microvascular pressures.[48] These measurements can be repeated several times over 1-6 h, allowing paired statistical comparisons of baseline and experimental states.[45]

After an isogravimetric state is obtained, venous pressure is elevated. The increase of lung weight demonstrates two distinct components: 1) a rapid component caused by fluid volume shifting into the pulmonary vascular system, and 2) a slow component that is due to fluid filtering across the pulmonary exchange vessels into the interstitial spaces. Weight gain is determined by drawing a tangent to the weight gain curve over each 1-min interval. The rate of lung weight gain can be estimated by logarithmic extrapolation to time zero, curve fitting, or measuring the weight gain slope at some time after the microvascular pressure increase.[45] In the time zero extrapolation method, these weight gain values are then plotted as a semilogarithmic function of time after the vascular pressure increase. By use of this method, the first 2 min of the curve are considered to represent vascular volume changes, whereas the slow increase in weight gain between 2 and 8 min represents transcapillary fluid movement. A least-squares line that best fit the natural log of slow weight gain between 2 and 8 min is extrapolated back to time 0 to determine the rate of fluid movement before any change in transcapillary Starling forces. Kfc values are normalized to 100 g initial lung wet weight and expressed as cm^3 per minute per mm Hg per 100 g by assuming that 1 g weight is equivalent to 1 ml of filtered fluid.

In our study the filtration coefficient is expressed in terms of the elevation of venous pressure. However, on sudden venous pressure elevation the resultant increase in capillary hydrostatic pressure is smaller than the change in venous pressure. This will result in some underestimation of the absolute magnitude of Kfc. The maximum possible variation is, however, smaller than 100%, because about half of the imposed venous pressure rise was measured to be even transmitted to the pulmonary artery.[49] Another methodological difficulty in measuring Kfc is inherent in all gravimetric approaches. An accurate estimate of gravimetric Kfc values requires differentiation of the weight gain due to intravascular volume changes from that due to transcapillary filtration. The intravascular volume increase is complete by 2 min after an increase in microvascular pressure and then weight gain increases at a decreasing rate.[50] A logarithmic extrapolation of the weight gain curve to time 0 to obviate the influence of tissue Starling forces readjustment has been recommended.[51] In contrary, Hancock et al. reported that the slow weight gain represents slow vascular volume changes that persists for about 20 min after a microvascular pressure increase.[52] Therefore,

Parker et al.[53] emphasize the necessity of maintaining the increased weight transient for 18–20 min to minimize errors due to vascular stress relaxation during baseline Kfc measurements and completely separate the vascular volume and filtration components of lung weight gain. Parker et al.[48] compared pulmonary Kfc values using measurements of transcapillary filtration rates based on laser densitometry and gravimetric measurement in isolated dog lungs. The authors found that Kfc values calculated by time zero extrapolation method were significantly higher than all other gravimetric or densitometric Kfc values. They concluded that small increases in Kfc may be obscured with use of the time zero extrapolation technique because of vascular stress relaxation persisting >3 min. However, in our models of pulmonary IR-induced injury lung vascular damage is so severe that the filtration component is considerably larger compared with the vascular volume component of lung weight gain, and therefore filtration rates can be measured using much shorter periods of weight gain.[53]

1.3. Oxidative stress in lung ischemia/reperfusion

Oxidative stress is characterized by an imbalance between prooxidants and antioxidants as a result of ROS overproduction that overwhelms the cellular antioxidant capacity.[54] Under physiological conditions, ROS are produced in a controlled manner at low concentrations and the rate of their production is balanced by the rate of elimination. However, under pathological conditions, excessive ROS production and an imbalance between ROS formation and the diminished ability to scavenge them by antioxidants results in increased bioavailability of ROS.[55-57] Increased levels of ROS cause oxidative damage of macromolecules, membranes, and DNA. Increased oxidative stress plays an important role in the pathophysiology of many diseases, including hypertension, atherosclerosis, diabetes, and ischemia/reperfusion.[18, 58]

Ischemia/reperfusion injury has been extensively studied in various organ systems, including intestines, kidney, liver, and heart.[59, 60] Much of this work suggests that ROS play a role in reperfusion injury[59] The increased generation of ROS during reperfusion contributes to tissue injury, microvascular dysfunction, increased endothelial permeability. Numerous experimental studies have demonstrated the therapeutic potential of antioxidant treatment in preventing or treating primary graft dysfunction after lung transplantation;[61] however, all clinical reports on the use of antioxidants are either case reports or case series. Thus, the role

of antioxidants in the treatment of primary graft dysfunction remains uncertain.[62] However, clinical trials of oral supplementation with antioxidant vitamins for the prevention of cardiovascular events in patients at risk for cardiovascular disease have generally been unsuccessful,[63, 64] suggesting that a therapeutic approach based on nonspecific ROS scavenging might be inappropriate. Selective inhibition of specific ROS-generating enzymes is another approach for reducing oxidative stress–induced tissue injury, although the exact molecular targets in lung IR have not yet been clearly defined.

1.3.1. Oxidative stress and biology of reactive oxygen species

ROS are formed as intermediates in reduction-oxidation processes.[65] Superoxide anion is a precursor for other ROS generated in cells. Its production usually involves a one-electron reduction of molecular O_2. Superoxide has an unpaired electron, which imparts high reactivity and renders it unstable and short-lived. Superoxide is poorly cell membrane permeable, but can cross cell membranes via anion channels.[66] It can undergo several chemical reactions depending on the amount generated and the localization and proximity to other radicals and enzymes. Superoxide acts as an oxidizing agent, where it is reduced to hydrogen peroxide.[65, 67] However, in pathological conditions, when produced in excess, it acts as a reducing agent and a significant amount of superoxide reacts with NO to produce a potentially deleterious peroxynitrite, also resulting in NO inactivation.[67]

Dismutation of superoxide by SOD produces the much more stable ROS, hydrogen peroxide.[65] Hydrogen peroxide is lipid soluble and crosses cell membranes. Hydrogen peroxide is then converted enzymatically into H_2O by catalase and glutathione peroxidise.[66] The interaction of hydrogen peroxide and superoxide in the presence of transition metal-containing molecules can yield the hydroxyl radical (Haber-Weiss reaction).[65] These reactions are often involved in oxidative stress-associated tissue injury. The hydroxyl radical is the one of the most deleterious and potent oxidizing agents known.

1.3.2. NADPH oxidases in ischemia/reperfusion

ROS can be detected during both ischemia[68] and reperfusion[18] and are believed to play a central role in IR injury. The ability of superoxide dismutase (SOD) to attenuate experimental IR lung injury suggests that superoxide anion is a key ROS in this process.[69] A major source of superoxide anion is the NADPH-dependent oxidase present in the plasma

membrane of PMN leukocytes.[70] Although there are many other enzyme systems that can potentially produce superoxide anion in the lung, including the uncoupled NO synthase, xanthine oxidase, cytochrome P450, and mitochondrial respiratory chain enzymes, the contribution of these enzymes to vascular generation of ROS is relatively minor compared with NADPH oxidase.[71] In addition, NADPH oxidase–derived ROS may promote and modulate oxygen radical production by other enzymes, thereby amplifying the total level of ROS.[58]

Though an NADPH oxidase plays important physiological roles in phagocytes it can also contribute to the pathogenesis of many inflammatory diseases.[72] Moreover, it has recently been shown that all vascular cell types (endothelial cells, vascular smooth muscle cells, and adventitial fibroblasts) produce ROS,[73, 74] primarily via NADPH oxidase.[55, 75, 76] A phagocyte-type NADPH oxidase expressed by endothelial cells is a predominant contributor to overall vascular ROS production; it has a specific critical role in vascular oxidative stress.[77] Furthermore, vascular NADPH oxidase–derived superoxide has been implicated in the pathophysiology of many cardiovascular diseases, including atherosclerosis, hypertension, diabetic vasculopathy and heart failure.[43]

Table 1. Tissue distribution of Nox enzymes. From Bedard and Krause, Physiol. Rev. 2007;87:245-313,[78] with modifications.

	High-Level Expression	**Intermediate- to Low-Level Expression**
Nox1	Colon	Smooth muscle, endothelium, uterus, placenta, prostate, osteoclasts, retinal pericytes
Nox2	Phagocytes	B lymphocytes, neurons, cardiomyocytes, skeletal muscle, hepatocytes, endothelium, hematopoietic stem cells, smooth muscle
Nox3	Inner ear	Fetal kidney, fetal spleen, skull bone, brain
Nox4	Kidney, blood vessels	Osteoclasts, endothelium, smooth muscle, hematopoietic stem cells, fibroblasts, keratinocytes, melanoma cells, neurons
Nox5	Lymphoid tissue, testis	Endothelium, smooth muscle, pancreas, placenta, ovary, uterus, stomach, various fetal tissues
Duox1	Thyroid	Airway epithelia, tongue epithelium, cerebellum, testis
Duox2	Thyroid	Salivary and rectal glands, gastrointestinal epithelia, airway epithelia, uterus, gall bladder, pancreatic islets

1.3.2.1. The NADPH oxidase family

The classical NADPH oxidase was first described and characterized in phagocytes, and it was originally thought that this system was restricted only to phagocytes and used solely in host defence. However, recently several isoforms of phagocytic NADPH oxidase, each encoded for by separate genes and termed Noxs, have been identified in nonphagocytic cells.[78] To date, the Nox family comprises five members (Nox1-5), of which Nox2 is gp91^{phox} or the phagocytic isoform. All Nox family members are transmembrane proteins that transport electrons across biological membranes to reduce oxygen to superoxide. In accordance with this preserved function, there are some conserved structural properties of Nox enzymes that are common to all family members.

1.3.2.2. Phagocytic NADPH oxidase

The phagocytic NADPH oxidase plays a crucial role in nonspecific host defence against pathogens by generating large amounts of superoxide during the so-called respiratory burst. The complex consists of a membrane-integrated heterodimeric flavoprotein cytochrome *b*558, which is itself composed of 2 subunits (gp91^{phox} and p22^{phox}) and 4 or more cytosolic proteins (p47^{phox}, p67^{phox}, p40^{phox} and a small regulatory protein GTPase Rac).[55]

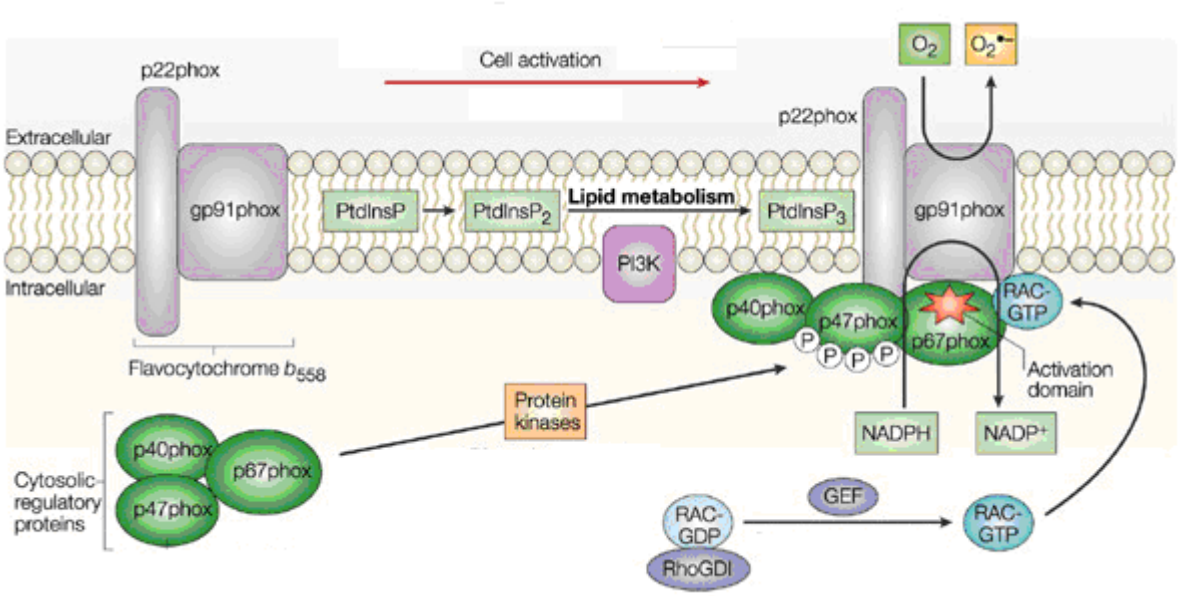

Figure 1. Activation of ROS generation by assembly of Phox regulatory proteins in phagocytes. From Lambeth, Nat Rev Immunol, 2004;4(3):181-9[79] with modifications.

Cytochrome *b*558 is considered to be the most important component of the complex with respect to both enzymatic stability and activity. In resting neutrophils, the NADPH oxidase is inactive but can be rapidly activated by various receptor-dependent and -independent stimuli (Fig. 1). Phosphorylation of $p47^{phox}$ upon cell stimulation leads to a conformational change allowing its interaction with $p22^{phox}$.[79] The cytosolic subunits form a complex that then migrates to the membrane, where it associates with the cytochrome *b*558 to assemble to an active form. Once assembled, the complex is active and generates superoxide by transferring an electron from cytoplasmic NADPH to extracellular or phagosomal oxygen to generate superoxide.

1.3.2.3. Endothelial NADPH oxidase

It is now well recognized that endothelial cells constitutively express a superoxide-generating enzyme analogous to the phagocytic NADPH oxidase of neutrophils. Several studies have suggested that, at a molecular level, the endothelial NADPH oxidase is similar to the phagocyte NADPH oxidase complex in that all the classical phagocytic oxidase subunits are expressed in endothelial cells.[75] Despite this similarity at a molecular level, there are significant functional differences between the phagocytic and endothelial NADPH oxidase. In particular, in contrast to the phagocytic enzyme, the endothelial oxidase is pre-assembled and constitutively active at a low level even in unstimulated cells, although its activity can be further increased by agonists.[80] Furthermore, it never generates a level of ROS comparable to the high burst activity of the phagocytic enzyme. Endothelial NADPH oxidase is regulated by many humoral factors, including cytokines, growth factors and vasoactive agents.[81] Physical factors, such as stretch, pulsatile strain and shear stress, also stimulate NADPH oxidase.[44]

1.3.3. Inhibitors of NADPH oxidase

The most commonly used NADPH oxidase inhibitor the iodonium-derivative diphenylene iodonium (DPI) represents a class of inhibitors of flavoprotein dehydrogenases that reduce activities of NADPH-dependent oxidase in the neutrophil and macrophage.[82, 83] The compound acts by abstracting an electron from an electron transporter and forming a radical, which then inhibits the respective electron transporter through a covalent binding step.[84] However, as suggested by the mechanism of action, DPI is a nonspecific inhibitor of all

flavoenzymes, including NO synthase,[85] xanthine oxidase,[86] mitochondrial complex I,[87] and others.[88].

4-(2-Aminoethyl)benzenesulfonylfluoride (AEBSF) is an irreversible serine protease inhibitor that inhibits NADPH oxidases by interfering with the association of the cytoplasmic subunit $p47^{phox}$.[89] It is not clear whether AEBSF really inhibits Nox enzymes or rather acts on signalling steps towards $p47^{phox}$ activation. AEBSF is also likely to have Nox-unrelated effects due to serine protease inhibition.[90] This mechanistic non-specificity and very weak potency of AEBSF make it unsuitable as a specific NADPH oxidase inhibitor.[91]

Several peptide-based inhibitors of NADPH oxidases have been reported. The peptide inhibitor gp91ds-tat was designed specifically to inhibit Nox2 by mimicking a sequence of Nox2 that is thought to be important for the interaction with $p47^{phox}$.[92] The ds-tat sequence allows for binding and membrane transport of the peptide into the cell. However, the peptide is a low-efficacy inhibitor, inhibiting neutrophil ROS generation by 25% at 50 μM.[92] Another peptide-based inhibitor of NADPH oxidases, PR-39, is an endogenous proline-arginine-rich antibacterial peptide secreted by neutrophils.[93] The peptide inhibits the phagocyte NADPH oxidase by preventing association of the p47phox regulatory subunit with p22phox.[93] However, PR-39 possesses antiadhesive properties by influencing some constitutive mechanisms involved in neutrophil trafficking,[94] and therefore can attenuate IR injury independently of inhibition of NADPH oxidase. In addition, PR-39 alters mammalian cell gene expression and behaviour.[95]

Apocynin (4-hydroxy-3-methoxy-acetophenone) is a naturally occurring methoxy-substituted catechol derived from the root extract of the medicinal herb Picrorhiza kurroa.[96] Picrorhiza kurroa has been used as a herbal medicine for centuries to treat inflammation and certain infectious diseases.[96] Apocynin has been shown to be a powerful anti-oxidant and anti-inflammatory agent in models of rheumatoid arthritis, inflammatory bowel disease, ischemic reperfusion lung injury, and respiratory muscle dysfunction in sepsis. The protective effects of apocynin are attributed to its ability to interfere with the assembly of enzyme subunits to form an active complex thereby preventing ROS generation.[97] This mechanism was also demonstrated in endothelial cells.[98] Apocynin has been used as an inhibitor of NADPH oxidases, both in neutrophils[97] and in endothelial cells.[99] It has recently been suggested that in non-phagocytic cells apocynin acts by functioning as a ROS scavenger, rather than an NADPH oxidase inhibitor and that it is therefore inappropriate to

use apocynin as a NADPH oxidase inhibitor in cells other than phagocytes.[100] The findings of Heumueller et al[100] question the results of many investigations showing the role of vascular NADPH oxidase as a major source of vascular ROS and oxidative stress. However, these conclusions were based on data derived from numerous studies that used various strategies to demonstrate the role of vascular NADPH oxidase.[101] Therefore, apocynin is now used indiscriminately as a valid Nox inhibitor.

1.3.4. Electron spin resonance spectroscopy

Establishing the precise role of ROS in normal physiological processes and in the development of diseases requires the ability to measure them and the oxidative damage that they cause. Numerous methods have been developed for their detection. The currently available methods include chemiluminescence techniques, fluorescence-based assays, enzymatic assays, and electron spin resonance (ESR) spectroscopy. Among these methods, ESR spectroscopy is a unique technique for detecting ROS in various systems, providing the most direct and specific measurement.

ESR spectroscopy is a technique for studying molecules that have one or more unpaired electrons, such as organic and inorganic free radicals or inorganic complexes possessing a transition metal ion. It deals with the interaction of electromagnetic radiation with the intrinsic magnetic moment of electrons arising from their spin. ESR detects the absorption of microwave energy, which occurs on transition of unpaired electrons in an applied magnetic field. The amplitude of the ESR signal is proportional to the number of the unpaired electrons present in the sample, allowing quantification of free radicals.

Most of the biologically relevant radicals are present in extremely low concentration and very short-lived, so it is difficult to directly detect them by ESR in biological samples. Therefore, for ROS measurement by ESR diamagnetic radical scavengers or spin traps have been used. These spin traps incorporate the radical into their structure, forming a long-lived paramagnetic adducts with specific ESR spectra. These products can accumulate to levels permitting detection by ESR spectroscopy. Spin traps can be used to both identify and quantify the original ROS. The most popular spin traps are the nitrone compounds such as DEPMPO and DMPO. Unfortunately, nitrone spin traps have a very low efficacy for trapping of superoxide radicals.[102] Furthermore, nitrone radical adducts are very susceptible to biodegradation and bioreduction to ESR silent species when exposed to biological

samples.[102] For this reason, it is impossible to accurately quantify radicals formed in biological systems using the currently available nitrone spin traps.

Recently, cyclic hydroxylamines were found to be effective scavengers of superoxide radicals.[103] In contrast to nitrone spin traps, they are effective scavengers of superoxide and produce a stable nitroxide radical.[104] Cyclic hydroxylamines, such as CPH or CMH, allow quantitative measurements of superoxide radicals with higher sensitivity than nitrone spin traps. Because these compounds can be oxidized by several ROS, it is necessary to perform paired experiments where SOD, a peroxynitrite scavenger, or other scavengers are added to define the ROS causing the reaction.

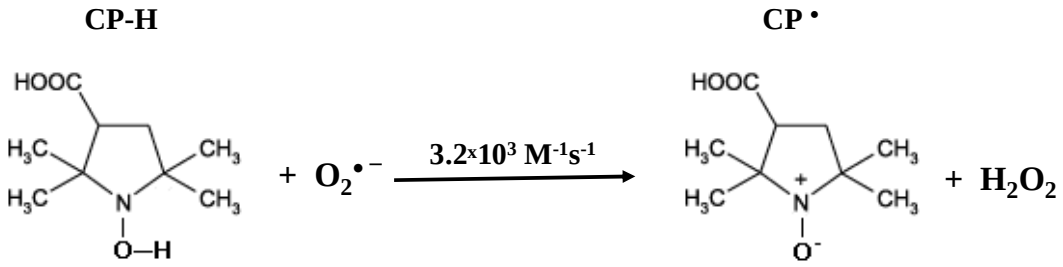

Figure 2. Reaction of CPH with superoxide. Oxidation of CPH forms the nitroxide $CP^{\bullet}$ radical. The reactions of cyclic hydroxylamines with $O_2^{\bullet-}$ are hundred times faster than those with nitrone spin traps, thereby enabling the hydroxylamines to compete with cellular antioxidants and react with intracellular $O_2^{\bullet-}$.

1.4. Aim of the study

Pulmonary IR results in endothelial damage and dysfunction leading to the development of high permeability pulmonary edema. A "burst" of ROS in the first several minutes of reperfusion has been observed by many investigators.[105] The first few minutes of reperfusion represent a critical phase because further tissue injury may be initiated at this time and most cell death occurs during reperfusion. Accordingly, therapeutic interventions must not only target specific cellular and molecular sources of ROS but also be delivered at precisely the right time. Thus, the present study aimed to investigate the role of phagocyte-type NADPH oxidase in the early phase of reperfusion. The relative contribution of NADPH oxidase expressed by resident leukocytes versus that from endothelial cells to IR-induced lung injury was also assessed.

2. Experimental protocols

Inclusion criteria for the study were *1*) a homogeneous white appearance of the isolated lungs with no signs of edema, hemostasis, or atelectasis; *2*) initial pulmonary arterial (Ppa) and ventilation pressure values in the normal range; and *3*) constancy of organ weight during an initial steady-state period of at least 20 min.

2.1. Ischemia/reperfusion protocols

2.1.1 Isolated lung preparations

After termination of the initial steady-state period and a control hydrostatic challenge for assessment of baseline vascular permeability, the lungs were exposed to ischemia for 240 min (rabbits) or 90 min (mice) by stopping the perfusion. The arterial and venous parts of the perfusion tubing were both clamped to maintain a positive intravascular pressure. During ischemia, the lungs were continuously ventilated with an anoxic gas mixture (95% N_2, 5% CO_2; Air Liquide, Deutschland GmbH, Ludwigshafen, Germany). At the end of the ischemic period, ventilation was returned to normoxia (21% O_2, 5% CO_2, 74% N_2; Air Liquide), and perfusion was re-established by increasing the flow stepwise over 3 min. Hydrostatic challenges were repeated 30, 60, and 90 min after the onset of reperfusion.

2.1.2. *In vivo* ischemia-reperfusion

After a left anterolateral thoracotomy, the pulmonary hilum of the left lung was occluded for 90 minutes using a noncrushing microsurgical clamp to create lung ischemia under the left lung in an inflated state. With removal of the clamp, the left lung was reperfused and reventilated for 90 minutes. Time-matched sham-operated WT and Nox2 KO animals served as controls. At the end of the reperfusion period, animals were sacrificed, and the left lungs were excised for assessment of tissue water content.

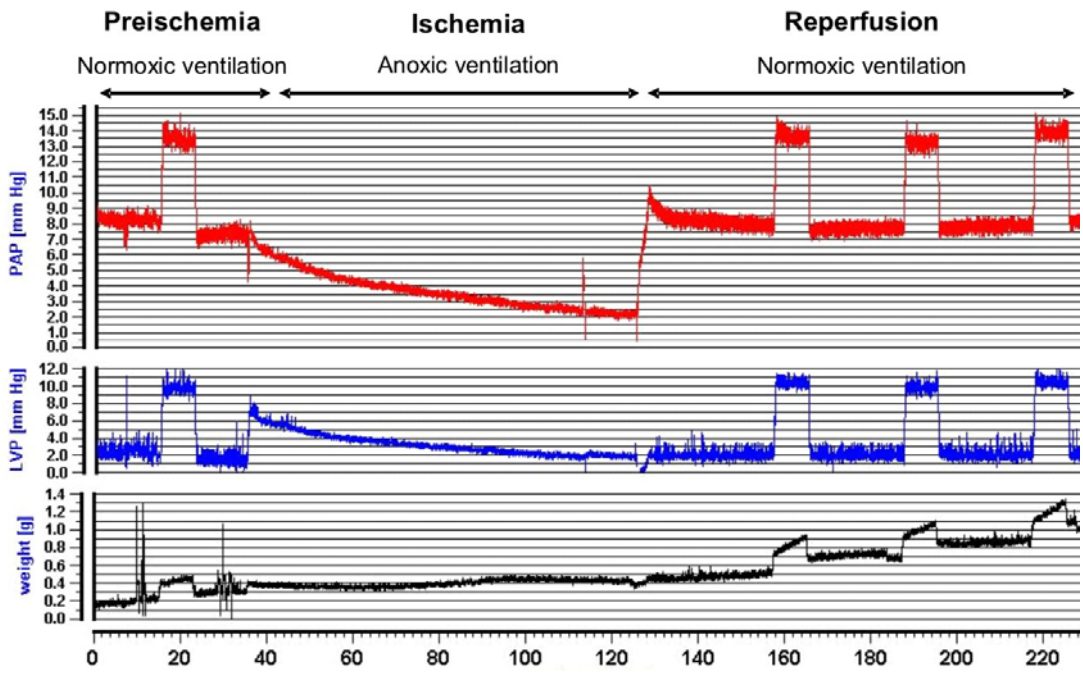

Figure 3. Representative original tracings of the isolated perfused mouse lung experiment. Typical tracings of pulmonary artery pressure, left ventricular pressure and weight changes in mouse lung reperfused after 90 min of lung ischemia induced by stopping perfusion.

2.2. Measurements of vascular permeability and lung weight gain

After termination of initial steady-state period a control hydrostatic challenge was performed, followed by anoxic ischemia. Hydrostatic challenges were then repeated 30, 60, and 90 min after the onset of reperfusion.

Rabbit experimental groups included untreated lungs and lungs treated with a NADPH oxidase inhibitor, apocynin (500 μmol/L; Sigma-Aldrich, Steinheim, Germany) or superoxide dismutase (SOD; 150 U/mL; Sigma-Aldrich) which were admixed to the perfusion buffer shortly before the onset of anoxic ischemia. In nonischemic control group untreated lungs were continuously perfused and normoxically ventilated throughout the experiment, and hydrostatic challenges were performed at time points corresponding to IR experiments.

Mouse experimental groups included lungs from wild-type (WT), Nox2 knockout (KO) and chimeric mice. Where indicated, an NADPH oxidase inhibitor, apocynin (500 μmol/L) or

SOD (150 U/mL) was admixed to the perfusion buffer of WT mouse lungs shortly before the onset of anoxic ischemia. In the time-matched non-ischemic control group, untreated lungs from WT mice were continuously perfused and normoxically ventilated throughout the experiment, and hydrostatic challenges were performed at time points corresponding to IR experiments.

2.3. Measurements of ROS production

In these experiments hand-made Teflon® cannulas were used in order to minimize contamination with transition metals of the perfusion buffer. After an initial steady state-period mouse lungs were exposed to anoxic ischemia. The spin probe, CPH (1 mmol/L in rabbit experiments and 0.5 mmol/L in mouse experiments), was added into the perfusate at the end of ischemic period 5 min before the onset of reperfusion. Samples from the venous outflow of the isolated lung were collected in 50-µL glass capillary tubes and measured immediately at room temperature. Samples were collected every 15 sec during the first 3 min of reperfusion and then every 1 min, or 5 min, as appropriate. Experimental groups included rabbit lungs and lungs from WT, Nox2 KO and chimeric mice. The contribution of superoxide radical to the formation of $CP^{\bullet}$ was determined in separate experiments performed in the presence of SOD in the buffer fluid (150 U/mL). In time-matched non-ischemic control lungs the spin probe was added, and perfusate samples were taken at time points corresponding to IR experiments.

3. Materials

3.1. Chemicals, injecting solutions and drugs

Isoflurane	Abbott, Wiesbach, Germany
Pentobarbital sodium (Narcoren)	Merial GmbH, Hallbergmoos, Germany
Heparin	Rathiopharm GmbH, Ulm, Germany
Physiological saline solution	DeltaSelect GmbH, Dreieich, Germany
Aqua B.Braun Ecotainer®	B.Braun Melsungen AG, Melsungen, Germany
Sodium bicarbonate 8.4%	Serag-Wiessner KG, Naila, Germany
Krebs-Henseleit electrolyte solution	Serag-Wiessner KG, Naila, Germany
Apocynin	Sigma-Aldrich, Steinheim, Germany
Baytril 2.5%	Bayer, Leverkusen, Germany
Superoxide dismutase from bovine erythrocytes	Sigma-Aldrich, Steinheim, Germany
EDTA	Fluka Biochemika, Buchs, Switzerland
RPMI1640	PAN Biotech GmbH, Aidenbach, Germany
Penicillin/Streptomycin	PAN Biotech GmbH, Aidenbach, Germany
Fetal calf serum	PAA Labortechnik, Pasching, Austria
Triton X-100	Merck, Darmstadt, Germany
Sucrose	Sigma-Aldrich, Steinheim, Germany
Magnesium chloride	Sigma-Aldrich, Steinheim, Germany
Tris-HCl	Sigma-Aldrich, Steinheim, Germany
Tween 20	Sigma-Aldrich, Steinheim, Germany
Nonidet P-40	Qiagen, Hilden, Germany
Proteinase K	Qiagen, Hilden, Germany
RED Taq DNA polymerase	Sigma-Aldrich, Hamburg, Germany
100bp DNA Ladder	Promega, Mannheim, Germany
Agarose (electrophoresis grade)	Fluka Biochemika, Buchs, Switzerland
Deoxy nucleotide mix (dNTPs)	Promega, Mannheim, Germany
Ethidium bromide	Sigma-Aldrich, Steinheim, Germany
Sodium chloride	Fluka Biochemika, Buchs, Switzerland
Potassium dihydrogen phosphate	Merk, Darmstadt, Germany
Potassium chloride	Fluka Biochemika, Buchs, Switzerland

Chelex 100 Resin	BioRad Laboratories, Hercules, CA, USA
Magnesium chloride hexahydrate	Fluka Biochemika, Buchs, Switzerland
Calcium chloride dihydrate	Fluka Biochemika, Buchs, Switzerland
D-(+)-glucose anhydrous	Fluka Biochemika, Buchs, Switzerland
Oncotic agent HAES®	Fresenius Kabi, Bad Homburg, Germany
DTPA	Sigma-Aldrich, Munich, Germany
NaOH	Merck, Darmstadt, Germany
CPH.Hydrochloride	Alexis Biochemicals, San Diego, CA, USA
Ketavet (Ketamin hydrochlorid)	Pfizer Pharma GmbH, Karlsruhe, Germany
Rompun 2% (Xylazin hyrdochlorid)	Bayer, Leverkusen, Germany
Acrylamide	Roth GmbH & Co. KG, München, Germany
TEMED	Roth GmbH & Co. KG, München, Germany
APS	Sigma-Aldrich, Saint Louis, Misouri, USA
β-mercaptoethanol	Sigma-Aldrich, Saint Louis, Misouri, USA
Methanol	J.T. Baker, Holland
Skim milk powder	Fluka Biochemika, Buchs, Switzerland
Sodium dodecyl sulfate	Roth GmbH & Co. KG, Munich, Germany
ECL Advance Western Blotting Detection Kit	Amersham, GE Healthcare UK Ltd, Buckinghamshire, UK
Bio-Rad Dc protein assay kit	Bio-Rad Laboratories, Hercules, USA
Anti-β-actin	Sigma-Aldrich, Saint Louis, Misouri, USA
iNOS, eNOS and nNOS	R&D Systems, Inc, Minneapolis, USA
Anti-mouse HRP	Promega, Mannheim, Germany
Anti-goat	Santa Cruz Biotechnology, Inc, Heidelberg, Germany
Endothelial Cell Growth Medium (+Funganose)	Promocell (Heidelberg, Germany)
HBSS Mg^{++}/Ca^{++}	Promocell (Heidelberg, Germany)

3.2. Consumables

Single use syringes Inject Luer®, 1 ml, 10 ml, 20 ml	Braun, Melsungen, Germany
BD Microlance needles 21G, 26G	Becton Dickinson, Heidelberg, Germany

Sterile gauze 5 x 4 cm	Fuhrmann Verbandstoffe GmbH, Munich, Germany
Single use gloves Transaflex®	Ansell, Surbiton Surrey, UK
Gauze balls size 6	Fuhrman Verrbandstoffe GmbH, Munich, Germany
Napkins	Tork, Mannheim, Germany
Threads Nr. 12	Coats GmbH, Kenzingen, Germany
Surgical threads non-absorbable ETHIBOND EXCEL®, size 5-0	Ethicon GmbH, Norderstedt, Germany
Surgical instruments	Martin Medizintechnik, Tuttlingen, Germany
Disposable feather scalpel	Feather Safety Razor Co, Ltd, Osaka, Japan
Pipette tips, blue, yellow, white	EPPENDORF, Hamburg, Germany
Tygon® lab tubing 3603	Cole-Parmer Instruments Company, Vernon Hills, Illinois, USA
Tracheal cannula	Hand-made
Cannula for pulmonary artery catheterisation	Hand-made
Cannula for left heart catheterisation	Hand-made
Combi-Stopper	Intermedica GmbH Kliein-Winternheim, Germany
Combitrans Monitoring-Set	B.Braun Melsungen AG, Melsungen, Germany
Cell Strainer nylon mesh, 40 µm, 100 µm	BD Biosciences, Bedford, USA
Heparinized microcapillary tubes	Hämacont, Heilbron, Germany
Disposable micropipettes intraMARK 50 µl	Blaubrand; Brand GmbH, Wertheim, Germany
Haematocrit sealing compound	Blaubrand; Brand GmbH, Wertheim, Germany
Filter papers	Whatman, Schleicher & Schuell GmbH, Dassel, Germany
Steritop Filter GP Express 0.22 µm	Millipore, Eschborn, Germany
PVDF	Pall corporation, East Hills, NY, USA

3.3. Composition of Krebs-Henseleit solution

Sodium chloride	120 mM
Potassium chloride	4.3 mM
Potassium dihydrogen phosphate	1.1 mM
Calcium chloride	2.4 mM
Magnesium chloride	1.3 mM
Glucose	13.32 mM
Hydroxyethylamylopectin (molecular weight 200,000)	5% (wt/vol)

Krebs-Henseleit solution was used as perfusion buffer. 24 mM of sodium bicarbonate was added to perfusion buffer in order to adjust pH at 7.35-7.45.

3.4. Systems and machines for animal experiments

Peristaltic pump REGLO Digital MS-4/12	Ismatech SA, Labortechnik-Analytik, Glattbrugg, Switzerland
Piston pump Minivent Type 845	Hugo Sachs Elektronik Harvard Apparatus, GmbH, March-Hugstetten, Germany
Transbridge BM4	World Precision Instruments, Berlin, Germany
Thermomix UB	Braun Melsungen, Melsungen, Germany
Frigomix1495	Braun Melsungen, Melsungen, Germany
Research Grade Isometric Force Transducer	Harvard Apparatus, Holliston, USA
Cole Parmer Masterflex Peristaltic Pump Easy-load 7518-10	Cole Parmer, Vernon Hills, IL, USA
Harvard respirator cat/rabbit ventilator 6025	Hugo Sachs Elektronik, March Hugstetten, Germany
Force Transducer Type U1A	Hottinger Baldwin Messtechnik, Fuchstal, Germany
Analog-to-digital transformer PCLD-8115 wiring terminal board Rev. A2	Advantech, Feldkirchen, Germany
Air heater Enda ET 1311	Enda, Horb a.N, Germany

Blood analyser ABL 330	Radiometer, Copenhagen, Denmark
PCR-thermocycler	Biometra, Goettingen, Germany
DNA/RNA Electrophoreis unit	Biometra, Goettingen, Germany
Chemie Genius Bio Imaging System	Syngene, Cambridge, UK
Neubauer hemocytometer	L-Optik, Berlin, Germany
Microlitre centrifuge cooled Mikro 200R	Andreas Hettich GmbH & Co KG, Tuttlingen, Germany
Centrifuge Rotina 46R	Andreas Hettich GmbH & Co KG, Tuttlingen, Germany
Magnetic stirrer Ret-Basic	IKA Labortechnik, Stauffen, Germany
MiniScope MS100	Magnettech, Berlin-Adlershof, Germany
SDS-PAGE electrophoresis system	Bio-Rad Laboratories GmbH, Munich, Germany
Semi-dry western blot system	Bio-Rad Laboratories GmbH, Munich, Germany
Shaker	Keutz Labortechnik, Reisskirchen, Germany

3.5. Software

MiniScopeControl, version 2.4.1, ©Dmitri Vashkevich
Data Acquisition Software LABTECH NOTEBOOK, version 10.1

4. Methods

4.1. Animals

All animal experiments were in accordance with institutional guidelines.

Male New Zealand Wight rabbits (body weight 2.8-3.5 kg) were used.

Male wild-type (WT) C57BL/6J mice (26–30 g) were purchased from Charles River Laboratories (Sulzfeld, Germany). Male Nox2 knockout (KO) mice (C57Bl/6.129S6-*Cybb*^{tm1Din}/J) were obtained from Jackson Laboratories (Bar Harbor, ME, USA).

Figure 4. Isolated perfused and ventilated mouse lung.

4.2. Isolated ventilated and perfused lungs

Isolated perfused and ventilated lungs have long been used by investigators interested in the physiological, biochemical, and metabolic aspects of this complex organ.[46] This technique has also been adapted to study pathomechanisms underlying IR injury. We employed warm ischemia in isolated perfused lungs as this model permits uncomplicated measurement of relevant physiological variables including vascular pressures, membrane permeability, and

fluid balance. In addition, cells in the isolated perfused lung are maintained in their "normal" anatomical and physiological associations and local physiological regulations are maintained in the organ. We took advantage of isolated mouse lungs as this model allows use of different genetically altered animals in order to identify the role of specific genes.

4.2.1. Isolation, perfusion and ventilation of rabbit lungs

The technique of isolated rabbit lung perfusion was performed as described[46] with modifications. Rabbits were deeply anesthetized with intravenous ketamine (30-50 mg/kg) and xylazine (6-10 mg/kg) and anticoagulated with intravenous heparin (1,000 U/kg body weight). A median incision was made in the center of the neck, and the trachea was exposed by blunt dissection and partially transected. Animals were then intubated via a tracheostoma and were room air ventilated (tidal volume, 30 ml; respiratory rate, 30 breaths/min; positive end–expiratory, 1 cm H_2O) with a Harvard respirator (cat/rabbit ventilator 6025, Hugo Sachs Elektronik, March Hugstetten, Germany).

After midsternal thoracotomy, the ribs were spread, and the right ventricle was incised, and a fluid-filled perfusion catheter was immediately placed into the pulmonary artery and secured with a ligature. Immediately after insertion of the catheter, perfusion (Cole Parmer Masterflex Peristaltic Pump Masterflex Easy-load 7518-10, Cole Parmer, Vernon Hills, IL, USA) with sterile ice-cold Krebs-Henseleit solution (Serag-Wiessner, Naila, Germany) was started, and the heart was cut open at the apex. In parallel with the onset of artificial perfusion, ventilation was changed from room air to a pre-mixed normoxic normocapnic gas mixture of 21% O_2, 5.3% CO_2, balanced with N_2 (Air Liquide, Deutschland GmbH, Ludwigshafen, Germany).

Next, the trachea, lungs, and heart were excised *en bloc* from the thoracic cage (without interruption of ventilation and perfusion) and were freely suspended from a force transducer to monitor lung weight gain. A second perfusion catheter with a bent cannula at its tip was introduced via the left ventricle into the left atrium and was fixed by suture in this position. Meanwhile, the flow was slowly increased from 20 to 100 mL/min (total system volume 250 mL). After rinsing the lungs with >1 L buffer to wash out blood, the perfusion circuit was closed for recirculation. Left atrial pressure was set at 2.0 mm Hg to ensure zone III conditions throughout the lung at end-expiration. The isolated, perfused lung was placed in a temperature-equilibrated housing chamber, and the whole system (perfusate reservoirs,

tubing, housing chambers) was heated to 37.5°C. Additionally, the inspiration loop of the ventilation system was connected to a humidifier and heated to 37.5°C.
Pressures in the pulmonary artery (Ppa), the left atrium and the trachea were registered by means of pressure transducers connected to the perfusion catheters via small diameter tubing and were digitised with an analog-to-digital converter, thus allowing data sampling with a personal computer. The transducers were calibrated at zero to the hilum level before every measurement.

4.2.2. Isolation, perfusion and ventilation of mouse lungs

The technique of isolated mouse lung perfusion was performed as described[106] with modifications. Mice were deeply anesthetised intraperitoneally with pentobarbital sodium (100 mg/kg body weight) and anticoagulated with intravenous heparin (500 U/kg body weight). A median incision was made in the center of the neck, and the trachea was exposed by blunt dissection and partially transected. Animals were then intubated via a tracheostoma and were room air ventilated (tidal volume, 300 µL; respiratory rate, 90 breaths/min; positive end–expiratory pressure, 3 cm H_2O) with a specific piston pump (Minivent Type 845; Hugo Sachs Elektronik, March-Hugstetten, Germany).

After midsternal thoracotomy, the ribs were spread, the heart was incised at the apex, the right ventricle was incised, and a fluid-filled perfusion catheter was immediately placed into the pulmonary artery and secured with a ligature. Immediately after insertion of the catheter, perfusion (REGLO Digital MS-4/12; Ismatec SA, Labortechnik-Analytik, Glattbrugg, Switzerland) with sterile ice-cold Krebs-Henseleit solution (Serag-Wiessner, Naila, Germany) was started. In parallel with the onset of artificial perfusion, ventilation was changed from room air to a pre-mixed normoxic normocapnic gas mixture of 21% O_2, 5.3% CO_2, balanced with N_2 (Air Liquide, Deutschland GmbH, Ludwigshafen, Germany).

Next, the trachea, lungs and heart were excised *en bloc* from the thoracic cage (without interrupting ventilation and perfusion) and were freely suspended from a force transducer to monitor lung weight gain. A second perfusion catheter with a bent cannula at its tip was introduced via the left ventricle into the left atrium. Meanwhile, the flow was slowly increased from 0.2 to 2 mL/min (total system volume: 15 mL). After rinsing the lungs with >20 mL buffer to wash out blood, the perfusion circuit was closed for recirculation. Left atrial pressure was set at 2.0 mm Hg. The isolated, perfused lung was placed in a

temperature-equilibrated housing chamber, and the whole system (perfusate reservoirs, tubing, housing chambers) was heated to 37.5°C.

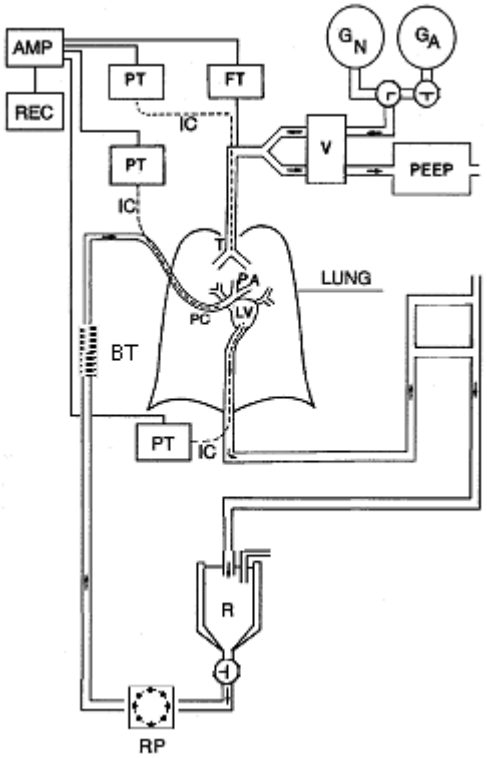

Figure 5. Schematic representation of the experimental set-up of the isolated perfused mouse lung. AMP - amplifier, BT – bubble trap, FT – force transducer, G_N – normoxic gas supply, G_N – anoxic gas supply, IC – intraluminal catheter, LV – left ventricle, PA – pulmonary artery, PC – perfusion catheter, PEEP – positive end-expiratory pressure, PT – pressure transducer, R – reservoir, RP – roller pump, REC – recording device, T – trachea, V – ventilator. From Seeger et al. Methods Enzymol. 1994;233:549-84 with modifications.

Pressures in the pulmonary artery (Ppa), the left atrium and the trachea were registered by means of pressure transducers connected to the perfusion catheters via small diameter tubing and were digitised with an analog-to-digital converter, thus allowing data sampling with a personal computer (Fig. 5). The transducers were calibrated at zero to the hilum level before every measurement.

4.2.3. Vascular compliance measurements

The vascular compliance (change in vascular volume per change in microvascular pressure) was calculated from the initial, rapid phase of weight gain, occurring within 1-2 min after onset of venous pressure elevation. Increase in the vascular compliance may signal increase

in the capillary surface area, which is a determinant of the microvascular pressure step-induced fluid filtration, since both the site of main capillary filtration and the capacity of the pulmonary circulation are located in the microcirculation. Significant rises of Kfc values in the absence of any augmentation of vascular compliance thus indicate that increased hydraulic conductivity of the microvascular walls and not increased capillary surface area was the predominant underlying event.[46]

4.2.4. Vascular permeability measurements

For assessment of lung vascular permeability we utilized the approach of the measurement of transvascular fluid filtration under conditions of hydrostatic challenge (capillary filtration coefficient), as described.[46] During this sudden venous pressure elevation by 7.5-mmHg for 8 min flow was maintained and ventilation was not interrupted. This maneuver induced an initial rapid weight gain (within 1 min), representing predominantly enhanced vascular filling, and a subsequent slow phase of weight gain, reflecting transvascular fluid filtration.

In control lungs and even most injured lungs, the rate of weight gain between 2 and 8 min after pressure elevation steadily decreases, due to rising interstitial pressure, counterbalancing the increase in microvascular filtration pressure. Therefore, time zero extrapolation of the slope of the weight gain curve was performed, using a semilogarithmic plot of the weight gain according to Taylor and Gaar (1969). The Kfc was then calculated by use of the extrapolated initial rate of fluid filtration, expressed in cubic centimetres per second per gram wet lung weight per millimeter Hg microvascular pressure increase (in terms of the elevation in venous pressure) $x10^{-4}$.

4.2.5. Assessment of pulmonary edema

In addition to the calculation of Kfc values, the hydrostatic challenge-induced net lung weight gain was assessed. Lungs were freely suspended from a force transducer for weight monitoring. Lung weight gain was calculated as the weight difference before and 5 min after each hydrostatic challenge maneuver. It reflects changes in the microvascular hydraulic conductivity.

4.3. Western Blot Assay

The lungs were removed and immediately frozen in liquid nitrogen. They were then homogenised in lysis buffer containing 50 mM tris-(hydroxymethyl)-aminomethane (Tris)/HCl (pH 7.6), 150 mM NaCl, 10 mM $CaCl_2$, 60 mM NaN_3, 0.1% wt/vol Triton X-100 and a cocktail of protease inhibitors (Complete™ Protease Inhibitor Cocktail Tablets; Boehringer, Ingelheim, Germany) using a tissue homogenizer. Homogenates were centrifuged at 13,000 rpm at 4°C for 30 minutes. The supernatants were measured for protein content using Dye Reagent Concentrate (Bio-Rad Laboratories, München, Germany). Extracts containing equal amounts of protein (60 μg) were denatured by boiling for 10 minutes in Laemmli's buffer containing β-mercaptoethanol and separated on 8% SDS-polyacrylamide gels at 100 V. The separated proteins were transferred to PVDF membranes with a semidry transfer unit at 115mA for 1 hour 15 minutes. The blots were blocked with 6 % non fat milk powder solution and developed with specific goat polyclonal IgG antibodies: eNOS and nNOS (R&D Systems, Inc, Minneapolis, USA), 1:1000 and mouse polyclonal IgG antibody: iNOS (R&D Systems, Inc, Minneapolis, USA), 1:1000 and donkey anti-goat HRP-labeled secondary antibody (Santa Cruz: 1:5000) for eNOS and nNOS and goat anti-mouse HRP for iNOS. The bands were visualized using an enhanced chemiluminescence ECL Plus Western blotting detection reagents (Amersham Biosciences, Freiburg, Germany) and quantified by densitometry (Syngene, VWR). Density values are expressed relative to the β-actin (Sigma-Aldrich) control level of each sample. All densities reported are means and SEM of four separate experiments.

4.4. Measurement of nitrite and nitrate in perfusate

Nitrite/nitrate levels were measured in the perfusate samples using Griess reagent according to manufacturer's instructions (Sigma, Germany). Perfusate probes were sampled from venous effluent, aliquoted, and frozen immediately, and stored at -20°C until measurement. For measurement, 100 μl of perfusate was mixed with 100 μl of Griess reagent, 10 min and then 100 μl vanadium chloride was added. After 35 min incubation at 37ºC, the light absorbance at 540 nm was measured. Concentrations of nitrite/nitrate were calculated by plotting of achieved values against a calibration curve. Calibration curves were generated by serial dilutions of sodium nitrite of known concentrations in the same buffer as used for experiments.

4.5. Ischemia-reperfusion in living mice

The WT and Nox2 KO mice were anaesthetized by an intraperitoneal injection of ketamine (100 mg/kg) and xylazine (8 mg/kg). During the experiment the depth of anesthesia was adjusted in accordance to the toe-pinch reflex. An additional dose of ketamine (30 mg/kg) was given when necessary. Mice were placed into a custom-made heating chamber (37°C) to maintain body temperature during the entire experiment. Endotracheal intubation with a 21-gauge atraumatic cannula was performed through a tracheotomy, and mechanical ventilation was initiated (130 breaths/min, 225 µL stroke volume, and a positive-end expiratory pressure of 2 cm H_2O) with an inspiratory oxygen fraction of 50% using a mouse ventilator MiniVent type 845 (Hugo Sachs Elektronik, March-Hugstetten, Germany). To compensate for possible fluid losses saline was administered at a rate of 0.2 ml/hour. The left thoracic wall was shaved and disinfected. After a left anterolateral thoracotomy through the third left intercostal space, all animals were given 500 IU/kg heparin intrapercutaneously. Five minutes after heparin administration the pulmonary hilum of the left lung, including the bronchus, pulmonary artery, and pulmonary vein, was occluded for 90 minutes using a noncrushing microsurgical clamp to create lung ischemia under the left lung in an inflated state. With removal of the clamp, the left lung was reperfused and reventilated for 90 minutes. In time-matched sham-operated animals served as controls, a thoracotomy was performed without occlusion of the hilum. At the end of the reperfusion period, animals were sacrificed, and the left lungs were excised for assessment of tissue water content.

4.6. Wet-to-dry lung weight ratio

As a measure of pulmonary edema formation, wet-to-dry lung weight ratios were determined for left lungs. For this purpose, total lung weight was measured before (wet weight) and after a 48-hour drying process at an oven (Fisher Isotemp, 65°C) (dry weight).

4.7. Generation of chimeric mice

To evaluate the relative contributions of NADPH oxidase expressed by resident leukocytes and phagocyte-type NADPH oxidase expressed by endothelial cells, we assessed the effect of selective reconstitution or inactivation of leukocyte NADPH oxidase on IR-induced lung injury.

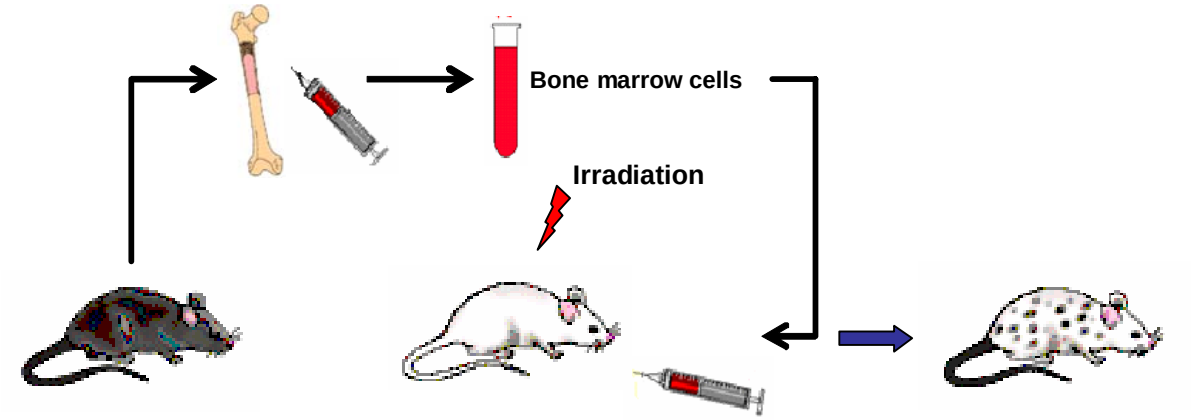

Figure 6. Schematic representation of chimeric mice generation.

4.7.1. Technique of bone marrow (BM) transplantation

Chimeric mice were produced as described[107] with modifications (Fig. 6). Donor mice (8 to 10 weeks old) were anticoagulated with an intraperitoneal injection of heparin (500 U) and then anesthetised by spontaneous inhalation of isoflurane and euthanized by cervical dislocation. After dissection of the femora and tibiae under the fume hood, the muscles were peeled off with sterile cotton swabs and the bones were put into cold medium on ice. Under the sterile cell culture hood bone ends were cut off with a scalpel. The bone shafts were then flushed with 21G needle on 5 mLl syringe with RPMI 1640 containing 1% FCS, 100 U/mL penicillin and 1000 U/mL streptomycin directly into 15 mL Falcon tube. The harvested bone marrow was centrifuged 5 min at 400xg at 4 °C. The supernatant was discarded and the pellet was resuspended in 1 mL medium by repeated pipetting and transferred into new Falcon tube through 100 µm nylon mesh. The cell strainer was rinsed with 1 mL medium. Afterwards the suspension was centrifuged 5 min at 400xg at 4 °C, the supernatant was

discarded and the cells were cooled on ice for 3 min. Subsequently, erythrocytes were lysed by adding 1 mL of ice-cold pure sterile water and gentle pipetting up and down 3-5 times. After 30 sec, 10 mL of cold medium were added. Next, the bone marrow was mechanically dissociated and filtered through a 40 µm nylon mesh to gain a single cell suspension. The cell suspension was then centrifuged 5 min at 400xg at 4 °C. The supernatant was discarded and the pellet was resuspended in 1 mL medium by repeated pipetting to produce a single cell suspension. Finally, the cells were counted using a Neubauer hemocytometer. About 5 x 10^7 mononuclear cells were harvested from each donor.

Recipient mice (8 to 10 weeks old) were BM depleted by lethal irradiation with an 1100-rad (11 Gray) ^{60}Co irradiator at a dose rate of ~0.6 Gray/min. Within 6–8 hr of irradiation, 2–5 × 10^6 donor BM cells in a volume of 150 µL sterile medium were injected into the lateral tail vein of the warmed recipient. BM reconstitution was allowed to occur for >3 months. During this time, chimeric mice were housed individually in sterile filter-isolator cages. Chimeras were administered Baytryl (10 mg/L; Bayer, Leverkusen, Germany) in sterile drinking water for 2 weeks, after which normal drinking water was used.

4.7.2. Types of chimeric mice

Three different groups of chimeras were generated (Fig. 7). To control for BM transplantation procedures, WT-to-WT chimeras (i.e., WT animals that received BM cells from WT mice) were generated, thus preserving NADPH oxidase function in all cells. In KO-to-WT chimeras, BM cells from Nox2 KO mice were transplanted into WT mice, resulting in selective inactivation of NADPH oxidase in BM-derived cells. In WT-to-KO chimeras, BM cells harvested from WT animals were transferred to Nox2 KO mice, resulting in selective reconstitution of NADPH oxidase in BM-derived cells.

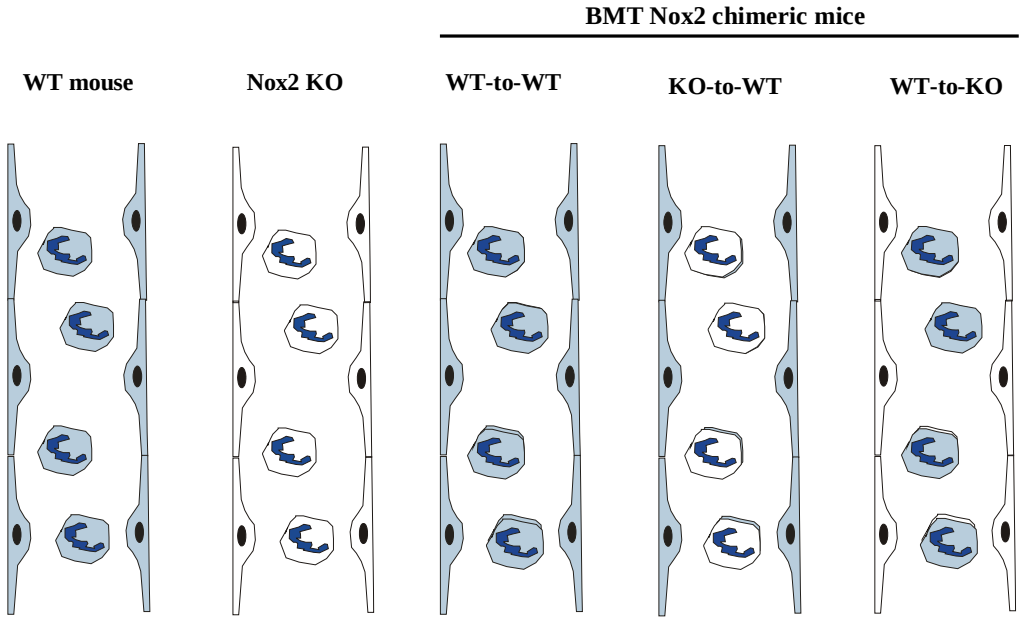

Figure 7. Schematic representation of Nox2 genotype in chimeric mice. Functional unaltered Nox2 allele is illustrated with dark coloured cells and disrupted Nox2 allele with white coloured cells. From left to right: WT mice, Nox2 KO mice, chimeric WT-to-WT mice (WT mice that received bone marrow cells from WT mice), KO-to-WT mice (WT mice that received bone marrow cells from Nox2 KO mice), WT-to-KO mice (Nox2 KO mice that received bone marrow cells from WT mice).

4.8. Genotyping of chimeric mice

The success of BM transplantation procedures was verified by PCR using genomic DNA obtained from blood cells or endothelial cells.

4.8.1. Isolation of genomic DNA from peripheral blood leukocytes

Genomic DNA of bone marrow derived cells was isolated from peripheral blood of chimeric mice. Blood (65−100 µL) was obtained from the lateral tail vein of mice with a heparinized microcapillary tube and expelled immediately into a 1.5 mL microfuge tube containing 20 µL of 10 mmol/L EDTA and mixed immediately to prevent clot formation. Blood was stored on ice until processing. Then 800 µL of lysis buffer A (0.32 mol/L Sucrose, 10 mmol/L Tris-HCl, pH = 7.5), 5 mmol/L $MgCl_2$, 1% v/v Triton X-100) was added to each tube and vortexed to suspend evenly. After microfuging at 1300xg for 15 min at 4 °C the supernatant was removed and nuclear pellet was resuspended in 1 mL of lysis buffer A. This

procedure was repeated two more times, or until no hemoglobin remained. After this steps nuclear pellet was resuspended in 100 µL of lysis buffer B (50 mmol/L KCl, 1.5 mmol/L $MgCl_2$, 10 mmol/L Tris-HCl, pH = 8.3), 0.45% NP-40, 0.45% Tween 20) with 100 µg/mL proteinase K and incubated at 55 °C for 120 min. After that the solution was heated to 97 °C for 10 min to inactivate proteinase K. This solution of genomic DNA was further used for PCR reaction.

4.8.2. Isolation of genomic DNA from endothelial cells

Genomic DNA of endothelial cells was isolated from aortic endothelial cells obtained from chimeric mice. Endothelial cells were collected after thorough washing of aortas with saline by scratching with a scalpel and were then put into 0.2 µL PCR tube with 50 µL of lysis buffer B and 100 µg/mL proteinase K. After incubation at 55 °C for 120 min the solution was heated to 97 °C for 10 min to inactivate proteinase K. This solution of genomic DNA was further used for PCR reaction.

4.8.3. Polymerase chain reaction

Genomic DNA obtained from peripheral blood cells or endothelial cells was amplified by PCR with two Nox2-specific primers and a neomycin-resistant primer (Metabion, Martinsried, Germany). The nucleotide sequences of the primers are listed in table 2. Primer pair oIMR0517 and oIMR0518 amplifies a 240-bp fragment from the wild-type allele. Primer pair oIMR0519 and oIMR0518 amplifies a 195-bp fragment from the disrupted allele.

Table 2. Nucleotide sequences of primers used for PCR.

oIMR0517	5'- AAg AgA AAC TCC TCT gCT gTg AA -3'	23-mer A=8, C=5, G=5, T=5
oIMR0518	5'- CgC ACT ggA ACC CCT gAg AAA gg -3'	23-mer A=7, C=7, G=7, T=2
oIMR0519	5'- gTT CTA ATT CCA TCA gAA gCT TAT Cg -3'	26-mer A=7, C=6, G=4, T=9

PCR was performed in a 25-µL reaction mixture containing 200 µmol/L dNTP, 1.5 mmol/L $MgCl_2$, 1 µmol/L DNA polymerase buffer, 2 U Taq polymerase (Invitrogen) and 0.4 µmol/L of each primer. Composition of the reaction mix for amplifying one sample is shown in table 3.

Table 3. Composition of 25 µL PCR mix for one sample

Reaction components	End volume, µL
10x PCR buffer	2.5
25 mmol/L $MgCl_2$	1.5
1 mmol/L dNTP	5.0
20 µmol/L primer oIMR0517	1
20 µmol/L primer oIMR0518	1
20 µmol/L primer oIMR0519	1
Template DNA	5
Red-Taq polymerase, 5 U/µL	1
Deionised water	7

All PCR reagents were mixed together in a 0.2 µL PCR tube, which was then placed in a thermal cycler (Biometra, Germany). The cycling conditions are shown in table 4.

Table 4. Cycling conditions for PCR

Step		Temperature	Time	Note
1	Denaturing	94°C	3 min	
2	Denaturing	94°C	20 sec	
3	Annealing	64°C	30 sec	-0.5°C per cycle
4	Elongation	72°C	35 sec	go to 2, 12 times
5	Denaturing	94°C	20 sec	
6	Annealing	64°C	30 sec	
7	Elongation	72°C	35 sec	go to 5, 25 times
8	Elongation	72°C	2 min	hold at 10°C

4.8.4. DNA agarose gel electrophoresis

Agarose gel electrophoresis was used for assessing amplified PCR products. Agarose powder was mixed with 1xTBE buffer (45 mmol/L Tris (pH 8.0), 45 mmol/L Boric acid and

2 mmol/L EDTA) and boiled in a microwave until agarose melted completely. Two µL of ethidium bromide were added into the solution and the gel was poured into a horizontal apparatus and polymerised for 20 min.

The PCR products were loaded onto the polymerised 2% agarose gel and placed in electrophoresis unit. The apparatus was then filled with 1xTBE buffer until it covered completely the gel. The gel was run at 110 Volt in gel electrophoresis. After electrophoresis, bands on the gel were visualized by Chemie Genius Bio Imaging System (Syngene, Cambridge, UK). The fragment size of amplified products was determined by comparing with the DNA molecular standard markers which were loaded along with the PCR products: 240 bp bands corresponded to fragments from wild type allele and 195 bp bands corresponded to fragments from disrupted allele.

4.9. Measurement of intravascular reactive oxygen species release

Measurement of ROS in intact organs is largely unresolved. Recently, we established a method combining ESR spectroscopy with the spin trapping technique for measurement of superoxide release from isolated perfused and ventilated lungs.[108]

4.9.1. Perfusion buffer preparation

For ESR measurements isolated mouse lungs were perfused with a modified Krebs-Henseleit solution, which was prepared with great care from the highest-grade chemicals to minimize contamination with transition metals. First, 120 mmo/L sodium chloride, 1.1 mmol/L potassium dihydrogen phosphate and 4.3 mmol/L potassium chloride were added to ultrapure water (Milli-Q, Millipore GmbH, Schwalbach, Germany). Then the solution was treated with 50 g/L chelator Chelex 100 Resin under constant stirring at room temperature for 4 hr. Afterwards the solution was first strained through filter paper (Whatman, Schleicher & Schuell GmbH, Dassel, Germany) using a funnel and then filter-sterilized (0.22 µm, Steritop, Millipore). After sterile filtration 2.4 mmol/L calcium chloride, 5 mmol/L glucose and 50 g/L hydroxyethyl starch (HAES) were added and stirred and then filter-sterilized. This solution was then kept at 4 °C until use in the experiments.

4.9.2. Spin probe preparation

Intravascular ROS release was measured by ESR spectroscopy using the spin probe 1-hydroxy-3-carboxy-2,2,5,5-tetramethylpyrrolidine (CPH; Alexis Corporation, San Diego, CA, USA), as described[108, 109] with modifications. Stock solutions of CPH (10 mmol/L) dissolved in 0.9% NaCl that contained 1 mmol/L diethylenetriamine-pentaacetic acid (DTPA) and was purged with argon were prepared daily and kept under argon on ice. DTPA was used to decrease CPH autooxidation, which is catalyzed by trace amounts of transition metals.

4.9.3. ESR spectroscopy settings

The ESR settings were as follows: microwave frequency 9.78 GHz, modulation frequency 100 kHz, modulation amplitude 2 G, microwave power 18 mW. More detailed information on ESR spectroscopy settings is provided in table 5.

Table 5. Parameters of ESR spectroscopy

Parameters	**Values**
B0-Field	3379.4G
Sweep width	58.52G
Sweep time	15 sec
Number	3
Smooth	0 sec (inactive)
Steps	4096
Modulation amplitude	2000mG
Power attenuation	10 dB
Receiver gain	500
Signal phase	180 (inversed)

4.9.4. ROS measurements

ESR samples were placed into 50 µl capillary tubes and measured at room temperature. Oxidation of the spin probe CPH by ROS leads to formation of the stable nitroxide radical 3-carboxy-proxyl ($CP^{\bullet}$). The amount of nitroxide formed is proportional to the concentration

of the reacted oxidant species. ROS formation was measured from the kinetics of nitroxide accumulation by following the ESR amplitude of the low-field component of ESR spectra. The rate of superoxide radical formation was determined by measuring the SOD-inhibited nitroxide generation in separate experiments performed in the presence of SOD in the buffer fluid (150 U/ml).

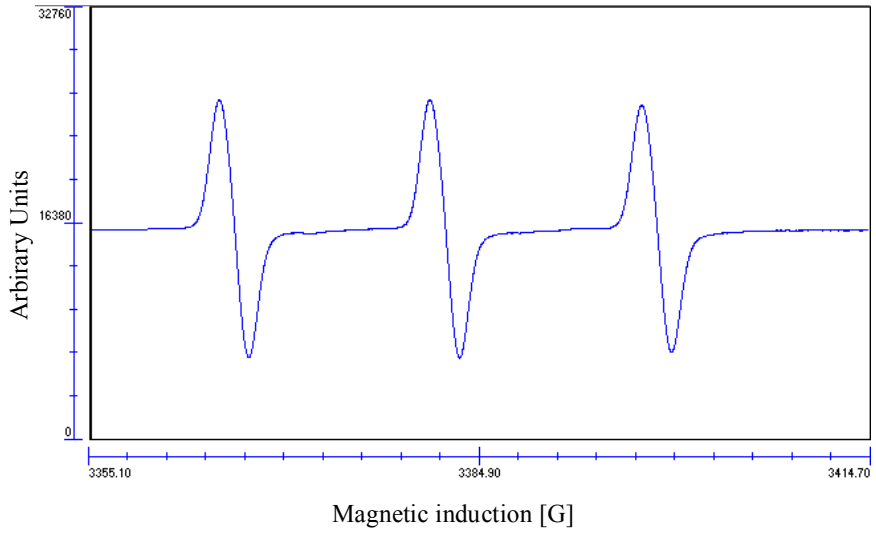

Figure 8. Typical ESR spectrum of $CP^{\bullet}$ nitroxide. The triple-line spectrum of $CP^{\bullet}$ radical resulting from the reaction of the spin probe CPH with ROS was detected using a MS 100 spectrometer (Magnettech, Berlin, Germany).

4.10. Endothelial cell culture

4.10.1. Isolation of human umbilical vein endothelial cells (HUVEC) from umbilical cord

The cord was laid on Petri dish and excess blood was dabbed off with gauze. Fresh cuts on both ends of the cord were made with a scalpel. At one end, a feeding needle was inserted carefully into the vein without damaging the surrounding tissue and fixed in place with a clamp. The umbilical vein was rinsed with 100 ml of HBSS Mg^{++}/Ca^{++} (Promocell). After clamping the other end of the vein, the cord was filled with collagenase until there was moderate distention of the vein. The cord was then incubated for 20 min. Afterwards, the cord was placed on a soft surface and gently massaged 2-3 times to facilitate cell detachment. The vein was washed with 30 ml of HBS and the cells were collected in a

prepared sterile 50 ml Falcon tube with 1 ml FCS. The Falcone tube was spinned at 1200 rpm for 5 min at room temperature. The supernatant was carefully aspirated, and the pellet of cells was resuspended in Endothelial Cell Growth Medium (+Funganose) (Promocell) and plated in a gelatinized 75 mm flask.

4.10.2. Anoxia-reoxygenation protocol in endothelial cell culture

After HUVECs reached 80% confluent, they were spitted on the gelatinized 30mm coverslips. The cells were incubated at 37°C with 5% CO_2 for 2 days. Coverslips were then placed in a 0.162 ml volume glass-covered perfusion chamber (Pecon, Germany), perfused (1 ml/min) with Hepes-Ringer buffer (HRB; 136.4 mmol/L NaCl, 5.6 mmol/L KCl/1 mmol/L $MgCl_2$, 2.2 mmol/L $CaCl_2$, 10 mml/L Hepes, 5 mmol/L glucose, pH 7.4) saturated with 21% O_2 (normoxia, $pO_2 \approx 150$ mmHg), and maintained at 37 ± 0.2°C by heating both the HRB and the chamber. Anoxia was induced by switching the perfusing HRB from normoxic to anoxic (continuously purged with 100% N_2). After a 90 min period of anoxia, reoxygenation was initiated by exposing the endothelial cells to normoxic HRB for 20 min. Time-matched control normoxic endothelial cells were exposed to normoxic HRB. Separate experiments from each study were performed with HUVECs from different human sources.

4.10.3. ROS measurement in endothelial cell anoxia-reoxygenation

Endothelial ROS release was measured by ESR spectroscopy using the spin probe CPH (Alexis Corporation, San Diego, CA, USA), as described with modifications.[109] Stock solutions of CPH (10 mmol/L) dissolved in 0.9% NaCl that contained 1 mmol/L diethylenetriamine-pentaacetic acid (DTPA) and was purged with argon were prepared daily and kept under argon on ice. DTPA was used to decrease CPH autooxidation, which is catalyzed by trace amounts of transition metals. The spin probe, CPH (1 mmol/L), was added into the HRB at the end of ischemic period 5 min before the onset of reperfusion. Samples from the outflow of the chamber with HUVECs were collected in 50-µL glass capillary tubes and measured immediately at room temperature. Samples were collected every 2 min starting 10 min before reperfusion and during reperfusion for 20 min.

4.11. Data analysis

Values are presented as the mean ± SEM. A Student's *t*-test was used to compare two groups. For multiple comparisons, a one-way analysis of variance followed by a Student-Newman-Keuls *post hoc* test was performed. $p < 0.05$ was considered statistically significant.

5. Results

5.1. Effects of ischemia and reperfusion on rabbit lungs

To investigate the role of NADPH oxidase in IR-induced lung injury, we assessed the effects of selective inhibition of NADPH oxidase on vascular permeability and intravascular ROS release in rabbit lungs.

5.1.1. Hemodynamic data

There were no significant differences in basal Ppa between different experimental groups. After 240 min of anoxic ischemia, a moderate and transient increase in Ppa followed by a decrease to baseline levels was observed upon reperfusion of rabbit lungs. Apocynin pre-treatment slightly suppressed the pressure response (Table 6).

Table 6. Pulmonary artery pressure in rabbit lungs.

	Ppa bas, mm Hg	Ppa rep, mm Hg
IR	6.8 (0.2)	16.8 (1.9)
Non-ischemic control	7.7 (0.1)	7.6 (0.2)
IR + apocynin	7.5 (0.3)	15.2 (0.9)

Data are presented as mean (SEM) of 4-6 independent experiments. Ppa bas – baseline pulmonary artery pressure before starting ischemia; Ppa rep – pulmonary artery pressure increase on reperfusion; IR – untreated lungs subjected to ischemia/reperfusion; non-ischemic control lungs were continuously perfused and normoxically ventilated; IR+apocynin – untreated lungs subjected to ischemia/reperfusion and pretreated with apocynin (0.5 mM).

5.1.2. Vascular compliance

Vascular compliance values were not significantly different between nonischemic control lungs and the different experimental groups and were virtually constant throughout the entire experimental period (Table 7).

Table 7. Vascular compliance in rabbit lungs.

	Vascular compliance, cm^3/mm Hg			
	Pre	Time after onset of reperfusion, min		
		30	60	90
IR	0.39 (0.04)	0.48 (0.01)	0.54 (0.01)	0.54 (0.01)
Non-ischemic control	0.51 (0.02)	0.52 (0.02)	0.55 (0.02)	0.57 (0.01)
IR + apocynin	0.55 (0.02)	0.48 (0.04)	0.62 (0.02)	0.61 (0.01)

Data are presented as mean (SEM) of 4-6 independent experiments. pre – baseline values before starting ischemia; IR – untreated lungs subjected to ischemia/reperfusion; non-ischemic control lungs were continuously perfused and normoxically ventilated; IR+apocynin – untreated lungs subjected to ischemia/reperfusion and pretreated with apocynin (0.5 mM).

5.1.3. Vascular permeability

In nonischemic rabbit lungs Kfc values were virtually constant throughout the entire experimental period. Ischemia and reperfusion resulted in increased microvascular permeability in untreated rabbit lungs. In parallel, massive edema formation was observed, and experiments had to be discontinued 60 min after the onset of reperfusion due to excessive fluid accumulation. Inhibition of the NADPH oxidase by apocynin significantly attenuated vascular leakage (Figure 9).

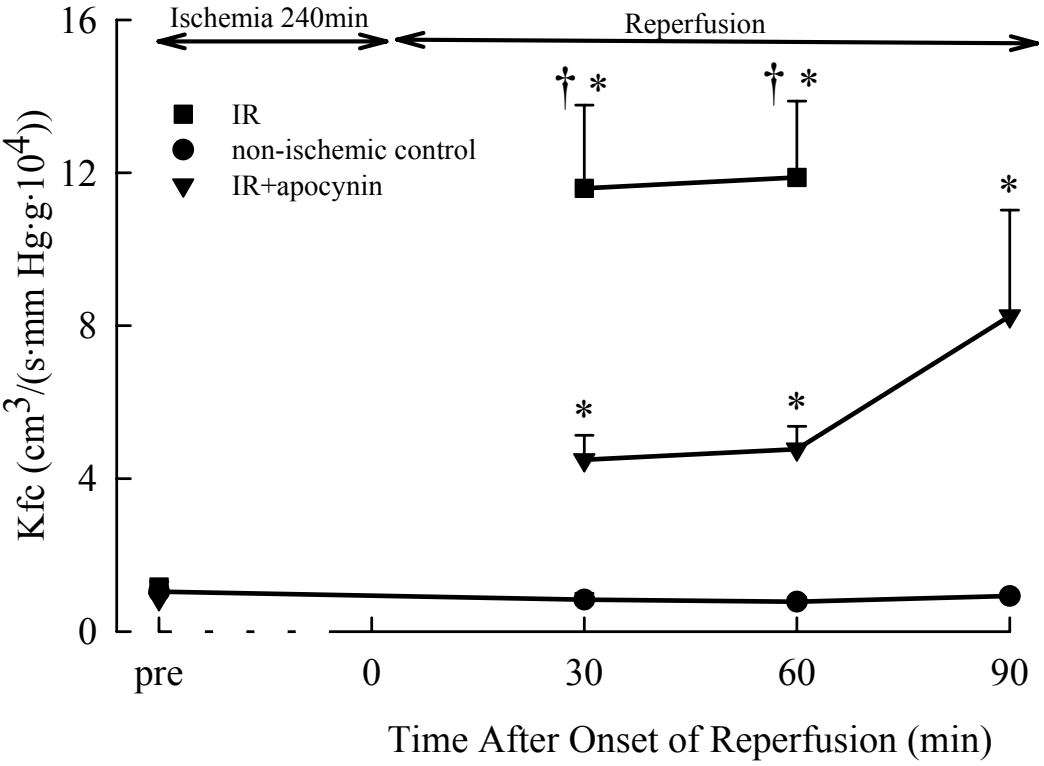

Figure 9. Vascular permeability in rabbit lungs. Lungs were exposed to anoxic ischemia for 240 min with following reperfusion. Time-matched non-ischemic control lungs did not undergo ischemia but were continuously perfused and normoxically ventilated. Kfc values were assessed, as described in Methods. Ischemia and reperfusion resulted in increased vascular permeability in lungs from the untreated IR group. Administration of apocynin significantly attenuated lung injury. Data are presented as mean ± SEM of 4-6 independent experiments. *p<0.05 compared with non-ischemic control group, †p<0.05 compared with IR+apocynin group. Kfc – capillary filtration coefficient; pre – baseline values before starting ischemia; IR – untreated lungs subjected to ischemia/reperfusion; IR+apocynin – untreated lungs subjected to ischemia/reperfusion and pretreated with apocynin (0.5 mM).

5.1.4. Pulmonary edema formation

In nonischemic rabbit lungs only marginal lung weight gain was observed throughout the entire experimental period. Ischemia and reperfusion induced massive edema formation in untreated rabbit lungs, and experiments had to be discontinued 60 min after the onset of reperfusion. Inhibition of the NADPH oxidase by apocynin significantly attenuated lung fluid accumulation (Figure 10).

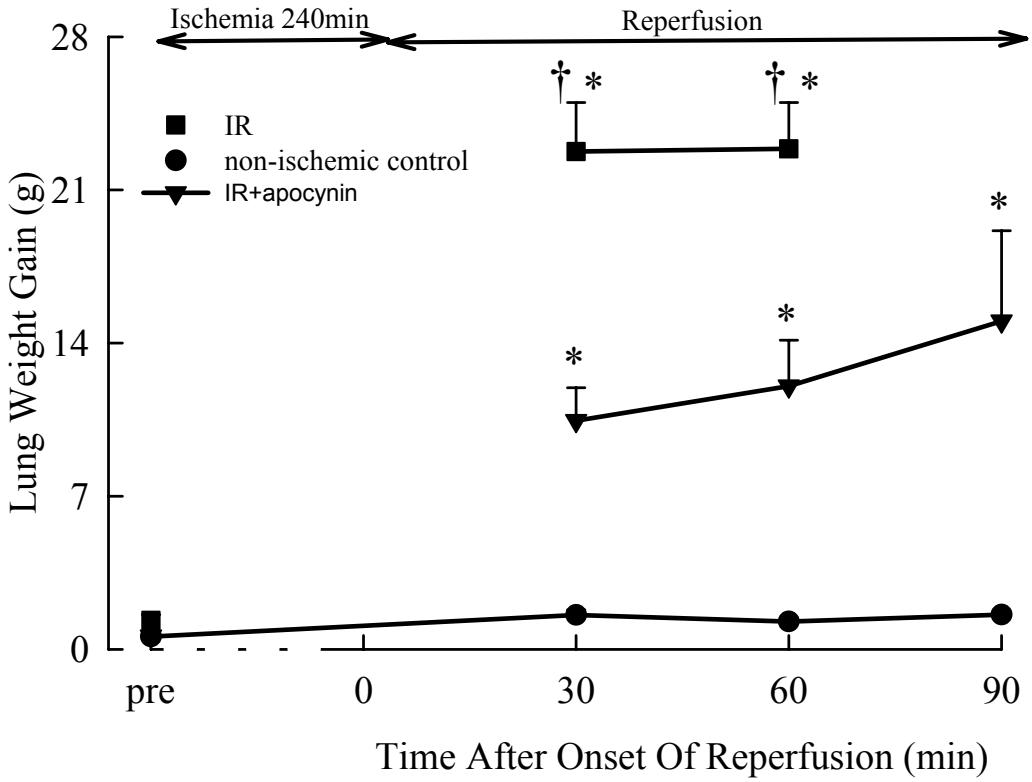

Figure 10. Lung weight gain in rabbit lungs. Lungs were exposed to anoxic ischemia for 240 min with following reperfusion. Time-matched non-ischemic control lungs did not undergo ischemia but were continuously perfused and normoxically ventilated. Lung weight gain was assessed, as described in Methods. Ischemia and reperfusion resulted in increased lung fluid accumulation in lungs from the untreated IR group. Administration of apocynin significantly attenuated vascular leakage. Data are presented as mean ± SEM of 4-6 independent experiments. *$p<0.05$ compared with non-ischemic control group, †$p<0.05$ compared with IR+apocynin group. pre – baseline values before starting ischemia; IR – untreated lungs subjected to ischemia/reperfusion; IR+apocynin – untreated lungs subjected to ischemia/reperfusion and pretreated with apocynin (0.5 mM)

5.1.5. Intravascular ROS release

Reperfusion of previously ischemic untreated rabbit lungs was associated with increased intravascular ROS release, when compared to nonischemic lungs. Parallel experiments in the presence of SOD revealed that the major portion of it was due to superoxide release. Inhibition of the NADPH oxidase by apocynin significantly reduced intravascular ROS release (Figure 11).

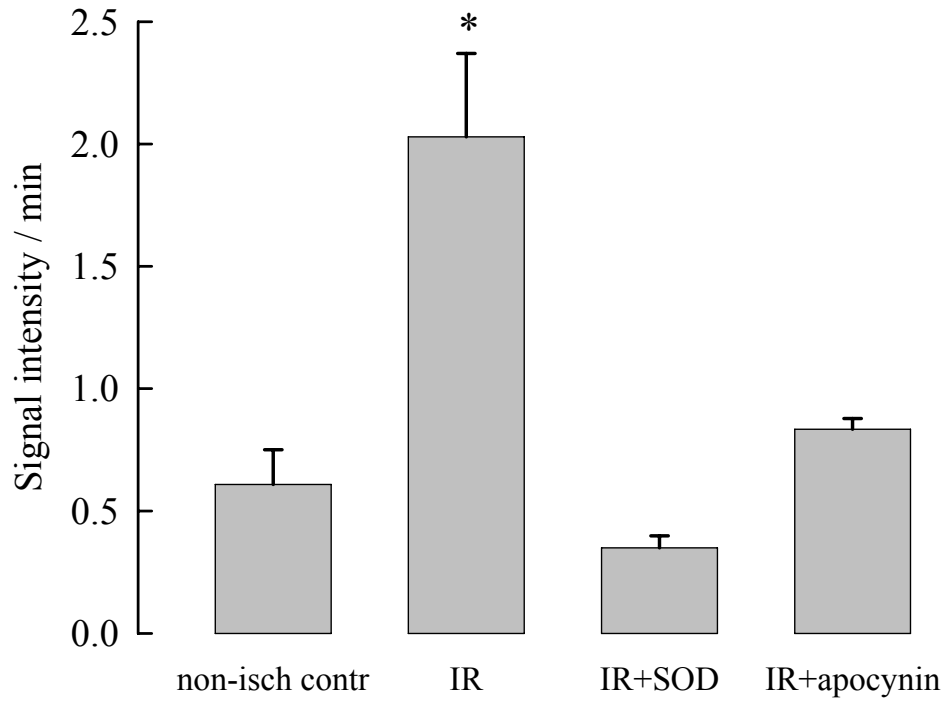

Figure 11. Intravascular ROS release in rabbit lungs. Lungs were exposed to anoxic ischemia for 240 min with following reperfusion. Time-matched non-ischemic control lungs did not undergo ischemia but were continuously perfused and normoxically ventilated. Spin probe CPH was added into perfusate 5 min before reperfusion. Samples from the venous outflow of the isolated lung were taken and measured immediately by ESR spectroscopy. The contribution of superoxide radical was determined in the presence of SOD in the buffer fluid. Increased ROS generation upon reperfusion of untreated IR lungs was reduced by SOD. Administration of apocynin decreased ROS generation as well. Data are presented as mean $\pm$ SEM of 4-6 independent experiments. *$p<0.05$ compared with all other groups. non-isch contr – non-ischemic control; IR – untreated lungs subjected to ischemia/reperfusion; IR+SOD – untreated lungs subjected to ischemia/reperfusion and pretreated with superoxide dismutase (150 U/ml); IR+apocynin – untreated lungs subjected to ischemia/reperfusion and pretreated with apocynin (0.5 mM).

5.2. Effects of ischemia and reperfusion on lungs from WT and Nox2 KO mice

To investigate the role of phagocyte-type NADPH oxidase in IR-induced lung injury, we assessed the effects of selective inhibition of NADPH oxidase and genetic deficiency of its catalytic subunit Nox2 on IR-induced injury in lungs from WT and Nox2 KO mice.

5.2.1. Hemodynamic data

There were no significant differences in basal Ppa between different experimental groups. In non-ischemic control lungs, pulmonary artery pressure values were essentially constant throughout the entire experimental period. After 90 min of anoxic ischemia, a moderate, transient increase in pulmonary artery pressure was followed by a decrease to baseline levels upon reperfusion of WT mouse lungs. Apocynin pre-treatment non-significantly suppressed the pressure response. In lungs from Nox2 KO mice the pressure response on reperfusion was attenuated to a similar extent (Table 8).

Table 8. Pulmonary artery pressure in WT and Nox2 KO mouse lungs.

	Ppa bas, mm Hg	Ppa rep, mm Hg
WT	8.1 (0.1)	11.6 (0.2)
Non-ischemic control	8.1 (0.2)	
WT + SOD	8.2 (0.2)	11.4 (0.4)
WT + apocynin	8.0 (0.3)	9.8 (0.3)
Nox2 KO	7.7 (0.1)	9.9 (0.2)

Data are presented as mean (SEM) of 4-6 independent experiments. Ppa bas – baseline pulmonary artery pressure before starting ischemia; Ppa rep – pulmonary artery pressure increase on reperfusion; WT – lungs from wild type mice subjected to ischemia/reperfusion; non-ischemic control lungs were continuously perfused and normoxically ventilated; WT+SOD – lungs from wild type mice subjected to ischemia/reperfusion and pretreated with superoxide dismutase (150 U/ml); WT+apocynin – lungs from wild type mice subjected to ischemia/reperfusion and pretreated with apocynin (0.5 mM); Nox2 KO – lungs from Nox2 knock-out mice subjected to ischemia/reperfusion.

5.2.2. Vascular compliance

Vascular compliance values were not significantly different between nonischemic control lungs and the different experimental groups and were virtually constant throughout the entire experimental period (Table 9).

Table 9. Vascular compliance in WT and Nox2 KO mouse lungs.

	Vascular compliance, cm^3/mm Hg			
	Pre	Time after onset of reperfusion, min		
		30	60	90
WT	0.01 (0.002)	0.01 (0.002)	0.01 (0.002)	0.01 (0.002)
Non-ischemic control	0.01 (0.001)	0.01 (0.001)	0.01 (0.001)	0.01 (0.001)
WT + SOD	0.01 (0.002)	0.01 (0.002)	0.01 (0.002)	0.01 (0.002)
WT + apocynin	0.01 (0.001)	0.01 (0.001)	0.01 (0.001)	0.01 (0.001)
Nox2 KO	0.01 (0.001)	0.01 (0.001)	0.01 (0.001)	0.01 (0.001)

Data are presented as mean (SEM) of 4-6 independent experiments. pre – baseline values before starting ischemia; WT – lungs from wild type mice subjected to ischemia/reperfusion; non-ischemic control lungs were continuously perfused and normoxically ventilated; WT+SOD – lungs from wild type mice subjected to ischemia/reperfusion and pretreated with superoxide dismutase (150 U/ml); WT+apocynin – lungs from wild type mice subjected to ischemia/reperfusion and pretreated with apocynin (0.5 mM); Nox2 KO – lungs from Nox2 knock-out mice subjected to ischemia/reperfusion.

5.2.3. Vascular permeability

There were no significant differences in baseline Kfc values among the different experimental groups (Figure 12). In non-ischemic lungs, Kfc values were essentially constant throughout the entire experimental period (Figure 12). Ischemia and reperfusion resulted in increased microvascular permeability in lungs from WT mice compared with time-matched non-ischemic control lungs (Figure 12). Inhibition of NADPH oxidase by apocynin as well as superoxide anion scavenging by SOD significantly attenuated vascular leakage (Figure 12). Similarly, lungs from mice with an NADPH oxidase deficiency (i.e., Nox2 KO mice) were protected against tissue injury (Figure 12).

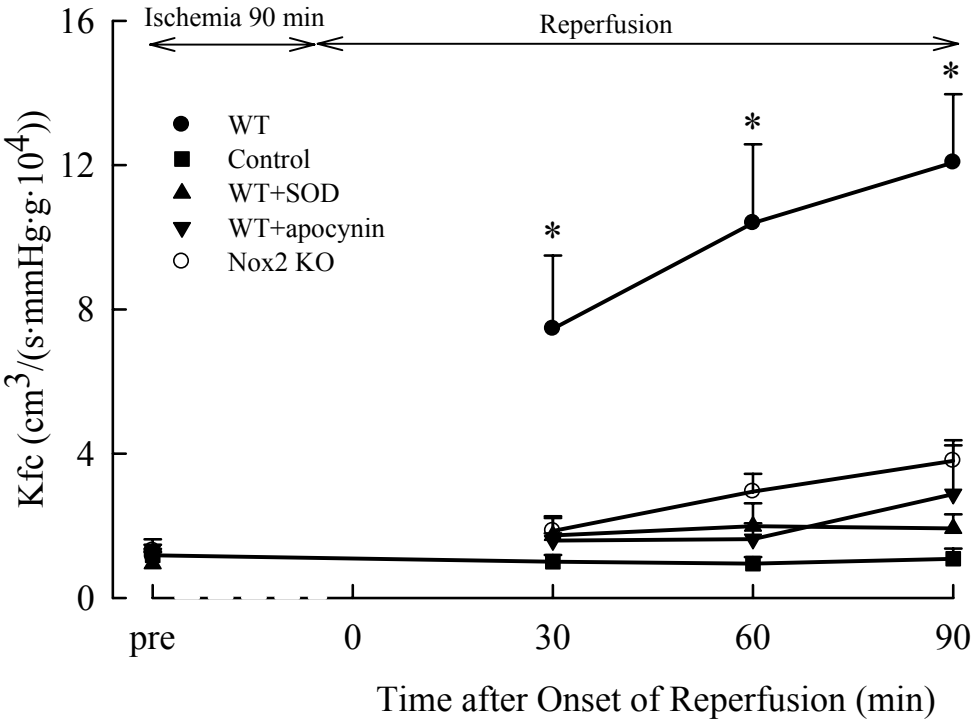

Figure 12. Vascular permeability in lungs from WT and Nox2 KO mice. Lungs were exposed to anoxic ischemia for 90 min with following reperfusion. Time-matched non-ischemic control lungs from WT mice did not undergo ischemia but were continuously perfused and normoxically ventilated. Kfc values were assessed, as described in Methods. Ischemia and reperfusion resulted in increased vascular permeability in lungs from WT mice. Pretreatment with apocynin as well as SOD significantly attenuated lung injury. Nox2 KO mouse lungs were protected against injury. Data are presented as mean ± SEM of 4-6 independent experiments. *$p<0.05$ compared with all other groups. Kfc – capillary filtration coefficient; pre – baseline values before starting ischemia; WT – lungs from wild type mice subjected to ischemia/reperfusion; WT+SOD – lungs from wild type mice subjected to ischemia/reperfusion and pretreated with superoxide dismutase (150 U/ml); WT+apocynin – lungs from wild type mice subjected to ischemia/reperfusion and pretreated with apocynin (0.5 mM); Nox2 KO – lungs from Nox2 knock-out mice subjected to ischemia/reperfusion.

5.2.4. Pulmonary edema formation

In non-ischemic lungs, only marginal lung weight gain was observed throughout the entire experimental period (Figure 13). Ischemia and reperfusion resulted in increased fluid accumulation in lungs from WT mice compared with time-matched non-ischemic control lungs (Figure 13). Inhibition of NADPH oxidase by apocynin as well as superoxide anion scavenging by SOD significantly reduced edema (Figure 13). Similarly, lungs from mice with an NADPH oxidase deficiency (i.e., Nox2 KO mice) were protected against tissue injury (Figure 13).

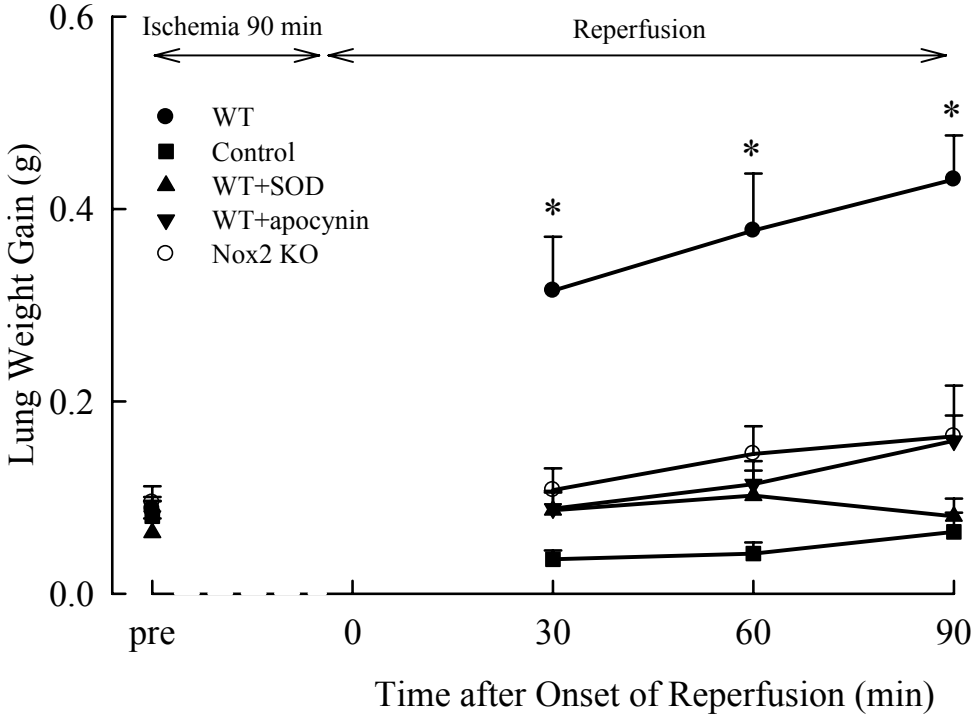

Figure 13. Lung weight gain in lungs from WT and Nox2 KO mice. Lungs were exposed to anoxic ischemia for 90 min with following reperfusion. Time-matched non-ischemic control lungs from WT mice did not undergo ischemia but were continuously perfused and normoxically ventilated. Lung weight gain was assessed, as described in Methods. Ischemia and reperfusion resulted in increased lung fluid accumulation in lungs from WT mice. Pretreatment with apocynin as well as SOD significantly attenuated vascular leakage. Nox2 KO mouse lungs were protected against injury. Data are presented as mean $\pm$ SEM of 4-6 independent experiments. *$p<0.05$ compared with all other groups. pre – baseline data before starting ischemia; WT – lungs from wild type mice subjected to ischemia/reperfusion; WT+SOD – lungs from wild type mice subjected to ischemia/reperfusion and pretreated with superoxide dismutase (150 U/ml); WT+apocynin – lungs from wild type mice subjected to ischemia/reperfusion and pretreated with apocynin (0.5 mM); Nox2 KO – lungs from Nox2 knock-out mice subjected to ischemia/reperfusion.

5.2.5. Intravascular ROS release

Reperfusion of previously ischemic lungs from WT mice was associated with increased intravascular ROS release as compared with time-matched non-ischemic control lungs (Figure 14). Parallel experiments in the presence of SOD revealed that the majority of ROS release was caused by superoxide (Figure 14). Inhibition of NADPH oxidase by apocynin significantly decreased ROS production (Figure 14). Moreover, in mice lacking Nox2, the catalytic NADPH oxidase subunit, intravascular ROS release was significantly attenuated (Figure 14).

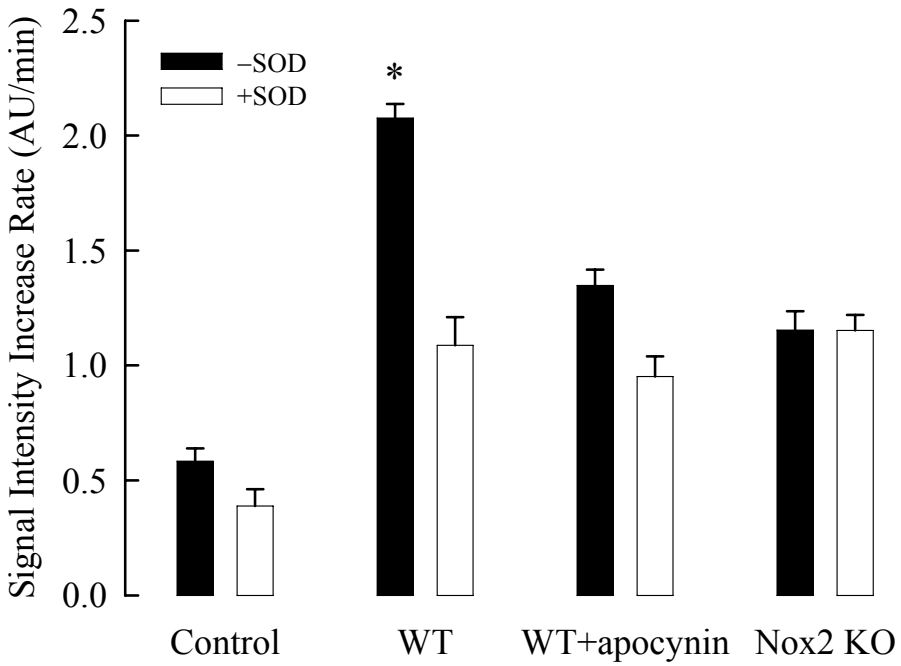

Figure 14. Intravascular ROS release in lungs from WT and Nox2 KO mice. Lungs were exposed to anoxic ischemia for 90 min with following reperfusion. Time-matched non-ischemic control lungs did not undergo ischemia but were continuously perfused. Spin probe CPH was added into perfusate 5 min before reperfusion. Samples from the venous outflow of the isolated lung were taken and measured immediately by ESR spectroscopy. The contribution of superoxide radical was determined in parallel experiments performed in the presence of SOD (150 U/ml) in the buffer fluid. Increased ROS generation upon reperfusion of WT mouse lungs was reduced by SOD and was attenuated in lungs from Nox2 KO mice. Data are presented as mean $\pm$ SEM of 4-6 independent experiments. *$p<0.05$ compared with all other groups. WT – lungs from wild type mice subjected to ischemia/reperfusion; non-isch contr – non-ischemic control; WT+apocynin – lungs from wild type mice subjected to ischemia/reperfusion and pretreated with apocynin (0.5 mM); Nox2 KO – lungs from Nox2 knock-out mice subjected to ischemia/reperfusion.

5.2.6. Expression of different NOS isoforms in lungs from WT and Nox2 KO mice

Baseline expression of eNOS and nNOS in lungs from Nox2 KO mice was not significantly different from that in lungs from WT mice (Figure 15). No baseline expression of iNOS was detected in lungs from WT and Nox2 KO mice (Figure 15).

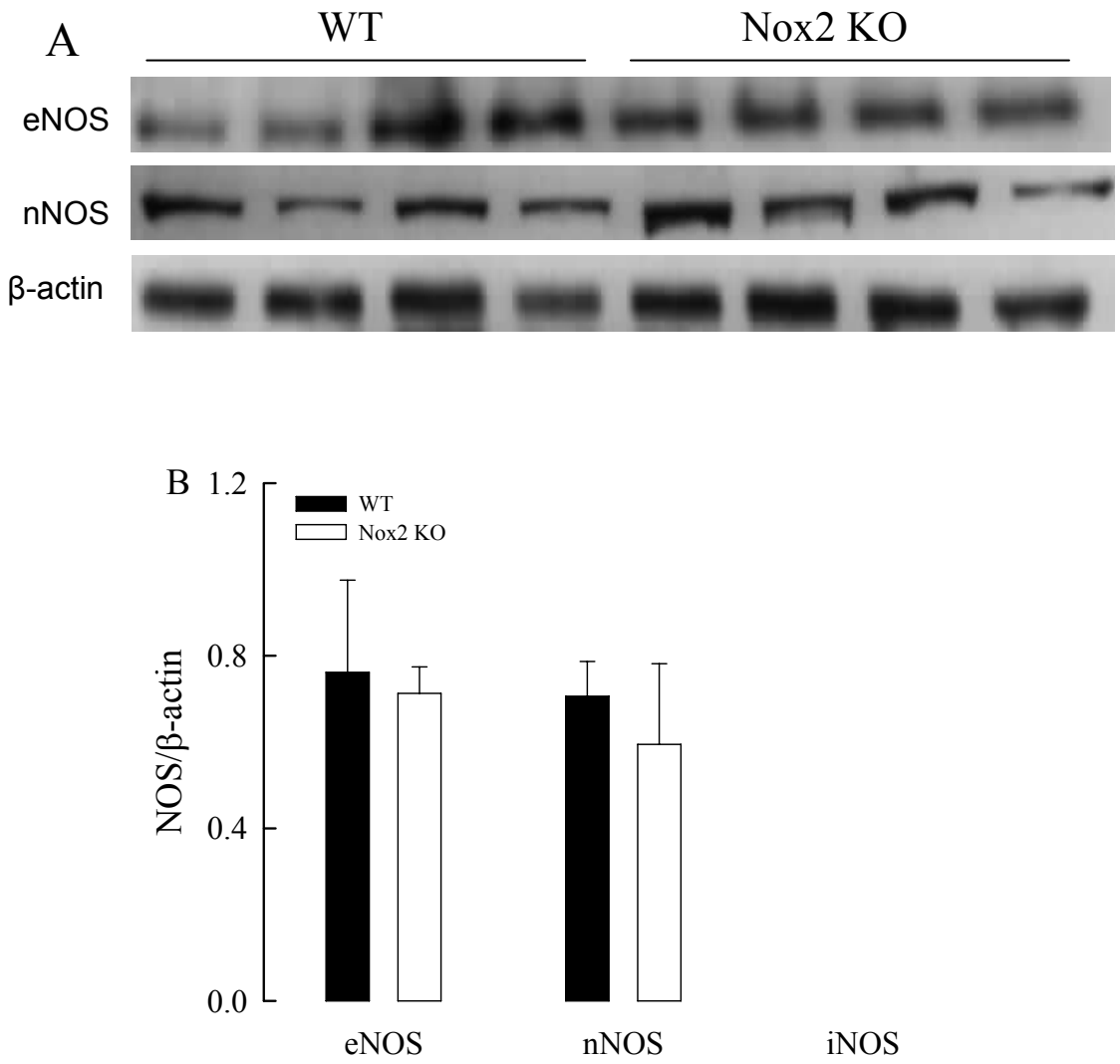

Figure 15. NOS expression in Nox2-deficiency. (A) Expression of NOS isoenzymes in lungs from WT and Nox2 KO mice. Proteins were extracted from the lungs and subjected to Western blot. (B) The bar graph illustrates the quantification of eNOS/nNOS expression levels normalized to β-actin levels. All data are presented as means ± SEM of 4 animals in each group.

5.2.7. NO production in lungs from WT and Nox2 KO mice

The levels of NO metabolites in Nox2 KO mice were not significantly different from those in WT animals (Figure 16).

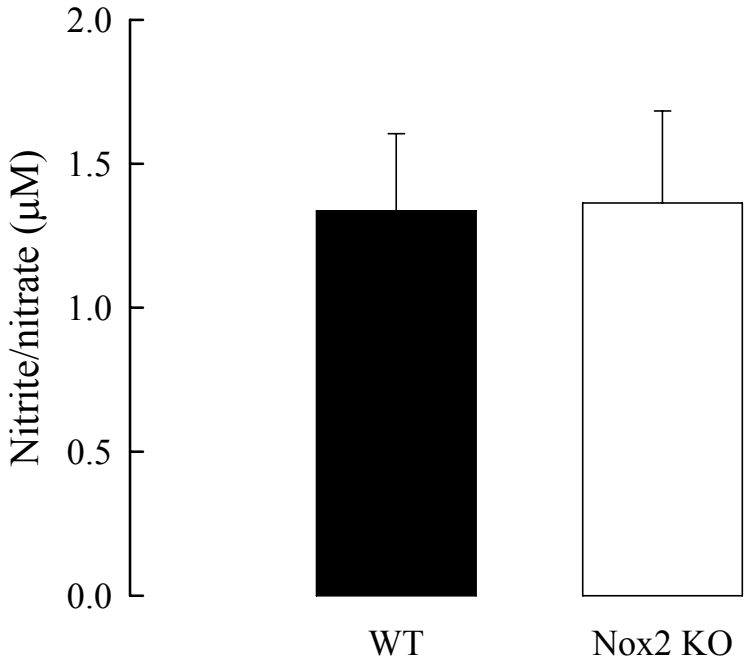

Figure 16. NO production in lungs from WT and Nox2 KO mice. All isolated lungs were continuously perfused and normoxically ventilated and perfusate samples were taken after perfusion for 30 min. Accumulation of NO metabolites was determined in perfusate samples by the Griess reaction. There were no significant differences in intravascular NO metabolites accumulation among the groups. Data are presented as mean ± SEM of 5-7 independent experiments.

5.3. Effects of lung ischemia and reperfusion in living WT and Nox2 KO mice

To further elucidate the pathobiological role of NADPH oxidase on IR-induced lung injury in an *in vivo* situation we investigated lung edema formation in anesthetized mice during ischemia-reperfusion. While WT mice developed severe edema, Nox2-deficient mice were completely protected (Figure 17).

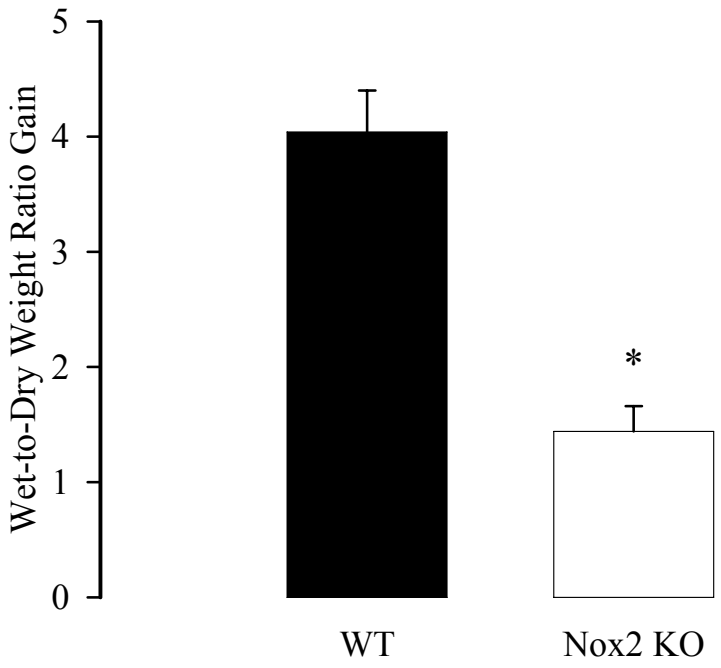

Figure 17. Pulmonary edema formation in living mice. Lung edema was analyzed by quantitative assessment of wet-to-dry weight ratios of ischemia-exposed lungs from wild-type (WT; n = 5) and Nox2-deficient (Nox2 KO; n = 5) mice which were normalized to sham-operated mice (n = 5 in each group). For ischemia left lungs were exposed to 1.5 hours of ischemia, followed by 1.5 hours of reperfusion. Values are given as mean ± SEM. * $P < 0.05$.

5.4. Characterization of chimeric mice

The efficiency of reconstituting BM-derived cells in chimeric mice was assessed by PCR 10 weeks after irradiation and transplantation. In all chimeric mice examined PCR band patterns of genomic DNA obtained from peripheral blood cells changed from the recipient pattern to donor pattern, indicative of successful reconstitution of bone marrow-derived cells by transplantation (Figure 18). Unaltered Nox2 allele was present in endothelial cells, as well as in leukocytes, of control WT-to-WT chimeric mice (Figure 18). In KO-to-WT chimeric mice, unaltered Nox2 allele was present in endothelial cells, whereas leukocytes contained a disrupted Nox2 allele (Figure 18). Conversely, in WT-to-KO chimeras, a disrupted Nox2 allele was present in endothelial cells, but leukocytes contained an unaltered Nox2 allele (Figure 18).

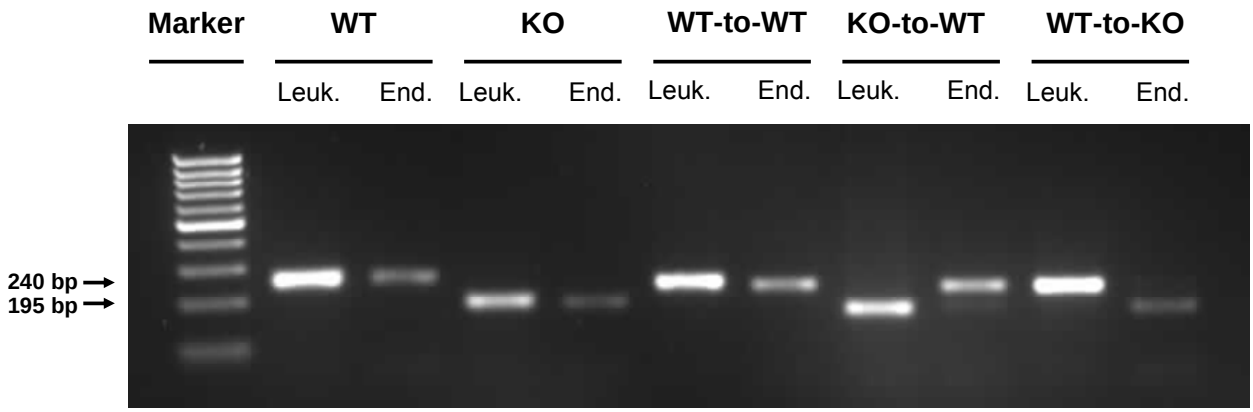

Figure 18. Genotypes in chimeric mice. WT, Nox2 KO and chimeric mice were genotyped by PCR using genomic DNA obtained from blood cells or endothelial cells with the Nox2-specific primers and the neomycin-resistant primer. WT = 240 bp, KO = 195 bp. In WT-to-WT mice in all cells unaltered Nox2 allele was present, similar to WT mice. In KO-to-WT mice unaltered allele was present in recipient endothelial cells, whereas in all donor bone marrow-derived cells disrupted allele was present. In WT-to-KO mice unaltered allele was limited to donor bone marrow-derived cells with disrupted allele present in recipient endothelial cells. Leuk. – leukocytes, End. – endothelial cells, WT – wild-type, KO – knock-out.

5.5. Effects of ischemia and reperfusion on lungs from chimeric mice

To evaluate the relative contributions of NADPH oxidase expressed by resident leukocytes and phagocyte-type NADPH oxidase expressed by endothelial cells, we assessed the effect of selective reconstitution or inactivation of leukocyte NADPH oxidase on IR-induced lung injury.

5.5.1. Hemodynamic data

A moderate and transient increase in pulmonary artery pressure was followed by a return to baseline levels upon reperfusion of lungs from chimeric mice (Table 10). Basal pulmonary artery pressure values and pressure responses after reperfusion did not differ significantly between the different experimental groups (Table 10).

Table 10. Pulmonary artery pressure in chimeric mouse lungs.

	Ppa basal, mm Hg	Ppa reperfusion, mm Hg
WT	8.1 (0.1)	11.6 (0.2)
WT-to-WT	8.1 (0.1)	11.4 (0.3)
KO-to-WT	8.4 (0.2)	11.3 (0.1)
WT-to-KO	8.2 (0.2)	10.8 (0.2)

Data are presented as mean (SEM) of 4-6 independent experiments. Ppa basal – baseline pulmonary artery pressure, Ppa rep – pulmonary artery pressure increase on reperfusion; WT – lungs from wild type mice subjected to ischemia/reperfusion; WT-to-WT – lungs from control chimeric mice; KO-to-WT – lung from chimeric mice with selective inactivation of NADPH oxidase in leukocytes subjected to ischemia/reperfusion; WT-to-KO – lungs from chimeric mice with selective reconstitution of NADPH oxidase in leukocytes subjected to ischemia/reperfusion.

5.5.2. Vascular compliance

Vascular compliances were not significantly different between WT mouse lungs and the different groups of chimeric mouse lungs and were virtually constant throughout the entire experimental period (Table 11).

Table 11. Vascular compliance in chimeric mouse lungs.

	Vascular compliance, cm^3/mm Hg			
	Pre	Time after onset of reperfusion, min		
		30	60	90
WT	0.01 (0.002)	0.01 (0.002)	0.01 (0.002)	0.01 (0.002)
WT-to-WT	0.01 (0.001)	0.01 (0.001)	0.01 (0.001)	0.01 (0.001)
KO-to-WT	0.01 (0.001)	0.01 (0.001)	0.01 (0.002)	0.01 (0.002)
WT-to-KO	0.01 (0.002)	0.01 (0.002)	0.01 (0.002)	0.01 (0.002)

Data are presented as mean (SEM) of 4-6 independent experiments. pre – baseline values before starting ischemia; WT – lungs from wild type mice subjected to ischemia/reperfusion; WT-to-WT – lungs from control chimeric mice; KO-to-WT – lung from chimeric mice with selective inactivation of NADPH oxidase in leukocytes subjected to ischemia/reperfusion; WT-to-KO – lungs from chimeric mice with selective reconstitution of NADPH oxidase in leukocytes subjected to ischemia/reperfusion.

5.5.3. Vascular permeability

Baseline Kfc values were similar among the different experimental groups (Figure 19). The severity of IR-induced increase in microvascular permeability in lungs from WT-to-WT and KO-to-WT chimeric mice was comparable to that in WT mouse lungs (Figures 12 and 19). In contrast, the dramatic rise in Kfc was significantly attenuated in lungs from WT-to-KO chimeric mice (Figure 19).

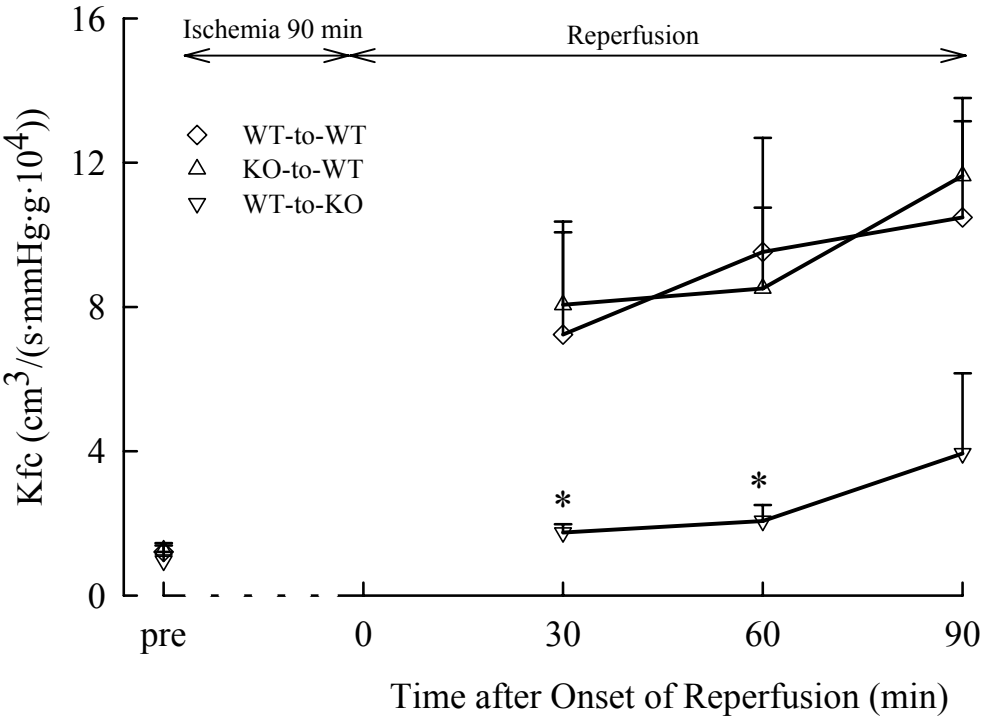

Figure 19. Vascular permeability in lungs from chimeric mice. Lungs were exposed to anoxic ischemia for 90 min with following reperfusion. Kfc values were assessed, as described in Methods. Ischemia and reperfusion resulted in increased vascular permeability in lungs from control WT-to-WT and KO-to-WT chimeric mice. In lungs from WT-to-KO chimeric mice the dramatic rise in Kfc was significantly attenuated. Data are presented as mean ± SEM of 4-6 independent experiments. *$p<0.05$ compared with all other groups. Kfc – capillary filtration coefficient, pre – baseline values before starting ischemia; WT – lungs from wild type mice subjected to ischemia/reperfusion; WT-to-WT – lungs from control chimeric mice subjected to ischemia/reperfusion; KO-to-WT – lung from chimeric mice with selective inactivation of NADPH oxidase in leukocytes subjected to ischemia/reperfusion; WT-to-KO – lungs from chimeric mice with selective reconstitution of NADPH oxidase in leukocytes subjected to ischemia/reperfusion.

5.5.4. Pulmonary edema formation

The severity of IR-induced edema in lungs from WT-to-WT and KO-to-WT chimeric mice was comparable to that in WT mouse lungs (Figures 13 and 20). In contrast, the severe fluid accumulation was significantly attenuated in lungs from WT-to-KO chimeric mice (Figure 20).

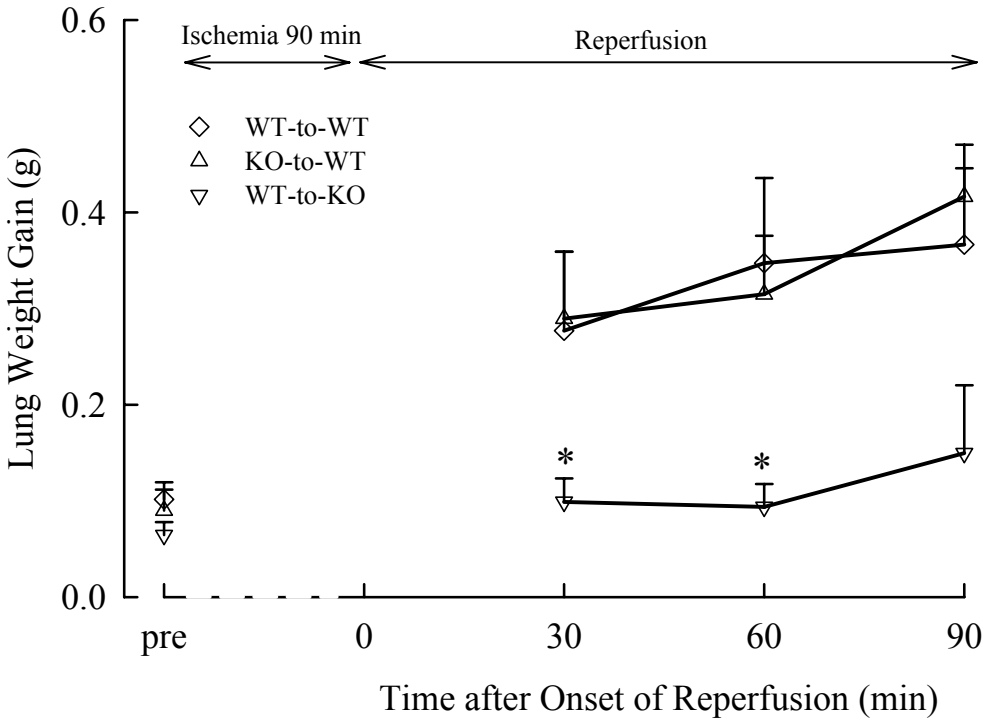

Figure 20. Lung weight gain in lungs from chimeric mice. Lungs were exposed to anoxic ischemia for 90 min with following reperfusion. Lung weight gain was assessed, as described in Methods. Ischemia and reperfusion resulted in severe lung edema formation in lungs from control WT-to-WT and KO-to-WT chimeric mice. In lungs from WT-to-KO chimeric mice fluid accumulation was significantly attenuated. Data are presented as mean $\pm$ SEM of 4-6 independent experiments. *$p<0.05$ compared with all other groups. pre – baseline values before starting ischemia; WT – lungs from wild type mice subjected to ischemia/reperfusion; WT-to-WT – lungs from control chimeric mice subjected to ischemia/reperfusion; KO-to-WT – lung from chimeric mice with selective inactivation of NADPH oxidase in leukocytes subjected to ischemia/reperfusion; WT-to-KO – lungs from chimeric mice with selective reconstitution of NADPH oxidase in leukocytes subjected to ischemia/reperfusion.

5.5.5. Intravascular ROS release

The reperfusion-induced increase in intravascular ROS release in previously ischemic lungs from WT-to-WT mice was comparable in magnitude to that in WT lungs (Figures 14 and 21). Parallel experiments in the presence of SOD revealed that the major portion of it was due to superoxide release (Figure 21). Attenuated intravascular ROS release was observed in the two other groups of chimeric mice (KO-to-WT and WT-to-KO; Figure 21).

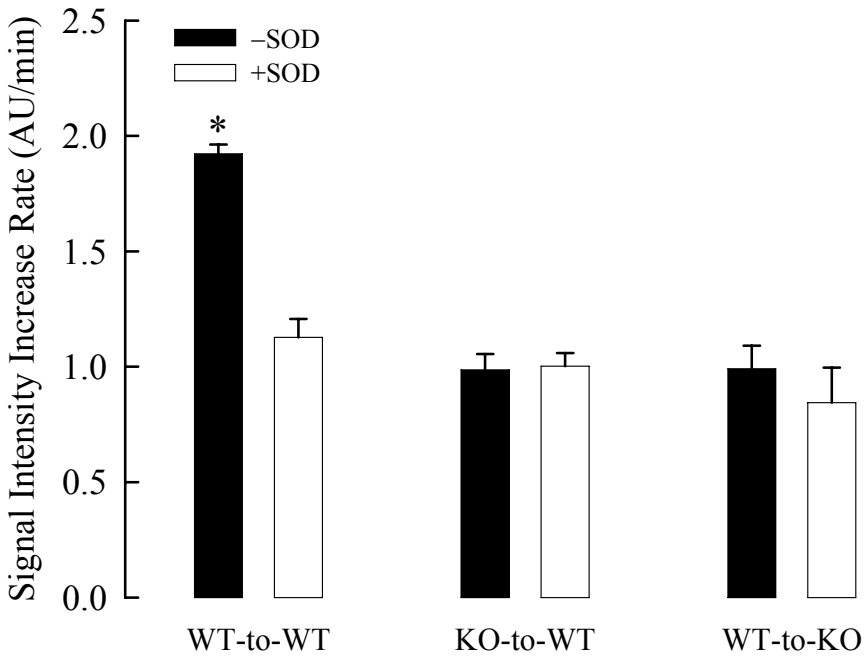

Figure 21. Intravascular ROS release in lungs from chimeric mice. Lungs were exposed to anoxic ischemia for 90 min with following reperfusion. Spin probe CPH was added into perfusate 5 min before reperfusion. Samples from the venous outflow of the isolated lung were taken and measured immediately by ESR spectroscopy. The contribution of superoxide radical was determined in parallel experiments performed in the presence of superoxide dismutase (SOD) in the buffer fluid (150 U/ml). Increased ROS generation upon reperfusion of lungs from WT-to-WT chimeric mice was reduced by SOD and was attenuated in lungs from KO-to-WT and WT-to-KO mice. Data are presented as mean $\pm$ SEM of 4-6 independent experiments. *$p<0.05$ compared with KO-to-WT and WT-to-KO mice. WT – lungs from wild type mice subjected to ischemia/reperfusion; WT-to-WT – lungs from control chimeric mice subjected to ischemia/reperfusion; KO-to-WT – lung from chimeric mice with selective inactivation of NADPH oxidase in leukocytes subjected to ischemia/reperfusion; WT-to-KO – lungs from chimeric mice with selective reconstitution of NADPH oxidase in leukocytes subjected to ischemia/reperfusion.

5.6. Effects of anoxia-reoxygenation on endothelial ROS production

Exposure of HUVEC monolayers to 90 min anoxia followed by 20 min reoxygenation resulted in significant increase in ROS production (Figure 22).

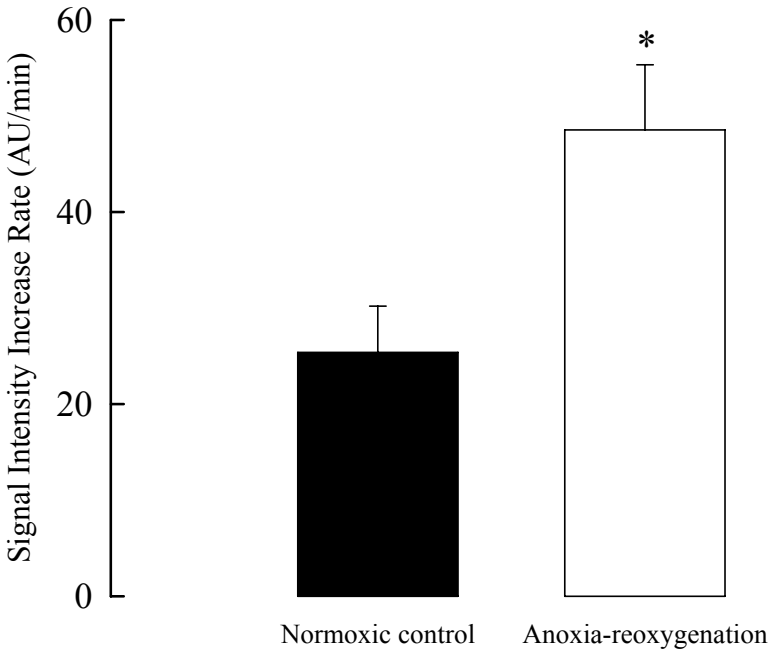

Figure 22. Effects of anoxia-reoxygenation on endothelial ROS production. Superoxide anion production by HUVECs submitted to normoxia or anoxia-reoxygenation measured by ESR spectroscopy. Data are presented as mean ± SEM of 4-6 independent experiments. *$p<0.05$ compared with normoxic control.

6. Discussion

In the present study we demonstrated that oxidative stress plays a role in lung IR injury by directly measuring enhanced intravascular ROS release from isolated perfused lungs from rabbits and WT mice. We also showed that ROS were derived from NADPH oxidase as pretreatment with apocynin, an NADPH oxidase inhibitor, significantly attenuated vascular injury after reperfusion of lungs from rabbits and WT mice. Moreover, tissue injury was significantly attenuated in lungs from mice lacking NADPH oxidase catalytic subunit Nox2. Furthermore, Nox2-deficient mice were completely protected from IR-induced lung injury in an *in vivo* situation. Finally, we demonstrated that endothelial, but not leukocyte, NADPH oxidase mediates lung injury during the early reperfusion phase.

6.1. Role of NADPH oxidase in ischemia/reperfusion-induced lung injury

We employed a model of warm ischemia in isolated lungs to induce a massive leakage response as reflected by severe pulmonary edema formation on reperfusion in lungs from rabbits and WT mice. A transient increase in Ppa was observed upon reperfusion of the lungs. The extent of this pressor response was rather limited as perfusion was re-established with gradual increase in flow. This pressure response could not account for the edema formation observed in the reperfused lungs, since Ppa increase was transient and returned to baseline levels in the majority of experiments. Moreover, the microvascular pressure levels measured in parallel with the permeability assessment in the same model were only marginally affected and did not significantly differ between the preischemic and postischemic hydrostatic challenge maneuvers.[110] Thus, the edema formation in the post-ischemic lungs in this model was independent of hydrostatic forces, and must be attributed to impaired pulmonary microvascular permeability, which was evident from the significant increase in the Kfc values. Although in lungs from Nox2 KO mice and in lungs from rabbits and WT mice treated with apocynin the pressure response was attenuated, this suppression was only moderate. In addition, the increase in Ppa followed by a decrease to baseline levels so that there were no significant differences between different groups in the Ppa values assessed at the time points of hydrostatic challenge for measurement of Kfc. Therefore, the protective effects of pharmacological inhibition of NADPH oxidase and NADPH oxidase

deficiency against IR lung injury must be primarily ascribed to maintenance of capillary endothelial barrier function.

In lungs from rabbits and WT mice, ischemia and reperfusion resulted in increased vascular permeability and edema formation associated with increased intravascular ROS release. Increased ROS generation during reperfusion after ischemia contributes to tissue injury, microvascular dysfunction, increased endothelial permeability and endothelial "stunning".[44] With respect to the lung, IR causes microvascular damage, an increase in capillary permeability, and acute pulmonary edema.[111] Previous efforts to clarify the source of ROS have, however, produced inconsistent results. Our observation that exogenously administered SOD attenuated IR-induced lung injury suggests that superoxide anions are critical for this process. This hypothesis is further supported by the observation that SOD also attenuated the ROS signal.

Although there are many enzymes that can potentially produce superoxide anions in the lung, including uncoupled NO synthase, xanthine oxidase, cytochrome P450 and mitochondrial respiratory chain enzymes,[71] the contribution of these enzymes to the vascular generation of ROS is relatively minor compared with NADPH oxidase. Numerous studies have shown that NADPH oxidase–derived ROS can promote and modulate oxygen radical production by other sources, thereby amplifying the total amounts of ROS.[58] Selective inhibition of NADPH oxidase with apocynin attenuated the IR-induced increase in pulmonary vascular permeability in lungs from rabbits and WT mice, demonstrating the role of NADPH oxidase in our model of ischemia and reperfusion. The selectivity of apocynin for NADPH oxidase has been well characterized.[97] Apocynin impedes the assembly of the $p47^{phox}$ and $p67^{phox}$ subunits within the membrane NADPH oxidase complex, thereby blocking formation of an active enzyme and preventing ROS generation.[97] In animal models, apocynin affords protection against IR-induced lung injury.[112, 113] Favorable effects of inhibiting NADPH oxidase were further confirmed by experiments with mice lacking Nox2, the main catalytic subunit of the enzyme, and in *in vivo* experiments. Reperfusion of isolated lungs from Nox2 KO mice was also associated with suppressed ROS production during the first minutes of reperfusion.

As superoxide reacts with nitric oxide (NO) and limits its bioavailability, reduced production of superoxide in Nox2 KO mice has been suggested to result in an increase in NO bioavailability[114]. In support of this idea, there is an increased 24-hour urinary excretion

of NO metabolites in conscious Nox2 KO mice.[115] Aortic segments from Nox2 KO mice exhibit a more pronounced endothelium-dependent relaxation to acetylcholine than that observed in aortae from WT animals.[114] The ROS scavenger tiron increases endothelium-dependent relaxation in WT mice, indicating that the reduced scavenging of endothelial NO by superoxide in the aorta from Nox2 KO mice could account for the enhanced relaxation.[114] Therefore, it is possible that increased bioavailability of NO could contribute to attenuation of lung injury in Nox2 KO mice. Alternatively, increased NO levels in Nox2 KO mice reported by some authors[115] might derive from compensatory changes in expression of enzymes producing NO.

Gene knockout approaches have helped to better understand the functions of different proteins. However, some results obtained from these knockout mice are unexpected and differ from the results of pharmacological intervention experiments. One possible explanation for this is that germ-line gene deletion with subsequent loss of function of a particular protein can induce changes in expression and/or function of other proteins with related function that can compensate for the loss of its function. For example, compensatory changes have been reported within the cAMP-dependent protein kinase system in mice deficient for specific cAMP-dependent protein kinase subunits.[116] The phagocyte NADPH oxidase is a critical component of innate immunity, responsible for generation of microbicidal ROS. The second genetically established antimicrobial mechanism of macrophages is production of reactive nitrogen species by inducible NO synthase (iNOS). There is evidence that NADPH oxidase and iNOS compensate for each other's deficiency in providing resistance to indigenous bacteria.[117] In addition, beneficial effects of NO and cGMP in lung IR have been reported[118, 119]. Macrophages from Nox2 KO mice produce more NO metabolites than WT animals,[120] supporting the idea of the potential compensatory changes in NADPH oxidase deficient mice.

To address these issues we compared expression and function of NO synthases in Nox2 KO mice with those in WT animals. We could not demonstrate any changes in baseline expression of constitutive NO synthases in lungs from Nox2 KO mice from that in lungs from WT mice. No baseline expression of iNOS was detected in lungs from WT and Nox2 KO mice Furthermore, the levels of NO metabolites in perfusate sample from Nox2 KO lungs were not significantly different from those in WT animals. Thus, we could not provide any evidence for compensatory changes in expression of NO synthases or increased

bioavailability of NO in Nox2 KO mice that might contribute to protection against IR lung injury.

The classical phagocyte-type NADPH oxidase was first described in neutrophils. Initially, this enzyme was thought to be a non-specific host defense mechanism against a variety of pathogens that was expressed specifically in phagocytes. NADPH oxidase has subsequently been shown, however, to have important physiological roles in phagocytes and also to contribute to the pathophysiology of many inflammatory diseases.[72] Circulating polymorphonuclear leukocytes play a pivotal role in IR lung injury[121-125]; yet the involvement of intrapulmonary resident leukocytes in oxidant lung injury remains controversial. It has recently been shown that the pulmonary capillary bed is the site of large marginated pools of leukocytes that contain 0.6–3 times the total number of circulating ones.[126, 127] Marginated neutrophils roll along the vessel wall, making transient contact with the endothelial cells without being firmly adherent.[128] Approximately 65% of the marginated neutrophils are in parenchymal vessels, primarily alveolar capillaries.[128] These large leukocyte populations display very slow washout kinetics even after extensive extracorporeal buffer perfusion,[129] assuming their role in reperfusion injury in isolated lung experiments.

Several different nonphagocytic cell types, including endothelial cells, vascular smooth cells and adventitial fibroblasts, constitutively express a superoxide-generating enzyme analogous to the NADPH oxidase of neutrophils.[55, 75, 130, 131] Moreover, a phagocyte-type of NADPH oxidase in endothelial cells is a major source of ROS production in endothelial cells[114] and is a predominant contributor to overall vascular ROS production.[77] Thus, endothelial cells or resident pulmonary leukocytes, or both cell types, may be the cellular source of the NADPH oxidase–derived superoxide anion during IR.

6.2 Role of endothelial NADPH oxidase in IR-induced lung injury

Although the late phase is dependent on neutrophil recruitment and activation, the early injury is neutrophil-independent and occurs by 15 minutes of reperfusion. As early injury occurs well before significant tissue neutrophil infiltration has occurred, it is likely dependent on lung resident cells.

To assess the contribution of NADPH oxidase from different resident cell types to IR-induced lung injury we used chimeric mice. Lungs from control chimeric animals (WT mice that received BM-derived cells from WT animals) exhibited IR-induced vascular injury comparable with that observed in lungs from WT mice, indicating that the irradiation and BM transfer procedures, per se, did not interfere with IR response. Selective reconstitution of NADPH oxidase on BM-derived cells in Nox2 KO mice did not abolish the protection afforded by a global deficiency of NADPH oxidase, in accordance with other reports that leukocytes are not essential for the initiation of IR injury.[29] Using an isolated rat lung perfusion model, Deeb et al.[28] demonstrated that ROS are involved in IR injury but neutrophils are not, because adding neutrophils did not enhance the injury. In addition, Dodd-o et al.[113] explored a genetic predisposition to lung IR in different mouse strains. Although they found that apocynin, an NAPDH oxidase inhibitor, attenuated lung injury, strain-dependent neutrophil–derived ROS production was not correlated with IR injury, suggesting that genetic differences in neutrophil NADPH oxidase activity do not determine the severity of IR injury.

Recently, it was demonstrated in an *in vivo* mouse model using chimeras created by BM transplantation between WT and p47phox KO mice that NADPH oxidase in BM–derived cells mediates pulmonary IR injury.[132] There may be several explanations for the discrepancy between our study and that of Yang et al. In contrast to our study, Yang et al. investigated the role of NADPH oxidase in IR lung injury using p47phox KO mice. Differential responses to different challenges in these two strains of NADPH oxidase KO mice have been reported. For example, a discrepancy in inflammatory response was observed between p47phox and Nox2 KO mice in response to chronic smoke exposure.[133] In addition, differential effect of p47phox and Nox2 deficiency on the course of pneumococcal meningitis has been demonstrated.[134] The reason for these differences is not clear but may be related to the activation of other vascular Nox enzymes by p47phox and/or different cellular distributions and functions of p47phox and Nox2 besides their role in ROS

production. In addition, we used a buffer-perfused model that eliminates contribution from circulating neutrophils and investigated the role of NADPH oxidase expressed in resident lung cells in early reperfusion. On the contrary, Yang et al.[132] demonstrated that NADPH oxidase–generated ROS from circulating BM-derived cells contribute to lung IR injury in the later phase of reperfusion. A biphasic pattern of IR injury was recently demonstrated, in which the first lung injury peak during early reperfusion was neutrophil independent and the second peak, in the later phase of reperfusion, was neutrophil mediated.[30] Finally, it is well known, that the severity of IR injury is determined by both the duration and the extent of blood flow decrease to an organ or tissue.[15] In the study of Yang et al. left lungs were exposed to 1 h ischemic period so that the injury might be much milder than that in our experiments. Therefore, the first peak of injury might be significantly diminished.

Our finding that resident leukocytes are not necessary to initiate lung injury, at least in the early phase of reperfusion, in isolated perfused mouse lungs does not, however, exclude the possibility that leukocytes might be primed by products produced during IR and may subsequently contribute to lung injury during later phases of reperfusion. ROS generated during endothelial hypoxia and reoxygenation stimulate MAP kinase signaling and kinase-dependent neutrophil recruitment.[135]

Thus, under transplant conditions, resident donor lung cells, rather than resident donor or circulating recipient leukocytes, may initiate IR injury. In support of this hypothesis, macrophages play a more important role in the early phase of reperfusion.[35, 39, 136] Depleting alveolar macrophages protects against lung IR injury, which supports a role for macrophages in the development of lung injury.[38] Macrophages can be depleted or inactivated by using clodronate liposomes or gadolinium chloride. However, it is well known that gadolinium salts can produce a wide variety of changes in physiology, because gadolinium chloride inhibits stretch-activated ion channels and physiological responses of tissues to mechanical stimulation.[137]. Liposome-encapsulated clodronate (clodronate-liposome) is transported into local macrophages by phagocytosis, and, after digestion, clodronate is released and induces cellular death. Clodronate-liposomes administered intratracheally have been used to deplete alveolar macrophages in some studies.[38-40]

Lung IR injury is associated with alterations in pulmonary surfactant composition and activity.[138] Pulmonary surfactant is a complex of macromolecular aggregates composed of phospholipids and surfactant proteins that is essential for maintenance of normal lung

function. Exogenous surfactant treatment before ischemia[139] or just before reperfusion improves the immediate lung transplant function in rats.[140] Intratracheally administered surfactant improves animal survival and decreases lung IR injury.[141, 142] Alveolar macrophage depletion with clodronate liposomes causes a severalfold increase in surfactant pool sizes in rats,[143] which underscores the role of alveolar macrophages in the catabolism of surfactant lipids and proteins.[144] Thus, surfactant accumulation after alveolar macrophages depletion may have important implications in the studies investigating the role of alveolar macrophages in lung IR injury and it may have contributed to the outcome of those studies.

NADPH oxidase deficient mice are characterized by slowly progressive late spontaneous lung emphysema development.[145] NADPH oxidase deficiency is also associated with increased influx of macrophages into the lungs with enhanced release of chemokines and cytokines.[133] Although, we used in our experiments NADPH oxidase deficient mice of younger ages before the development of lung emphysema, one would expect augmented tissue injury in lungs from Nox2 KO mice. On the contrary, these mice displayed marked protection against IR-induced lung injury, thus excluding the potential involvement of macrophages in the induction of the injury in our model.

Macrophages and neutrophils are both reconstituted after BM transplantation, and they share the same genotype in reciprocal chimeras.[146] Sixty days after total body irradiation and BM transplantation, most resident lung alveolar macrophages are of donor origin,[147] thus excluding their role as a ROS-generating source during the induction of lung injury in the WT-to-KO chimeric mice in our study.

Selectively inactivating leukocyte NADPH oxidase by transplanting BM-derived cells from Nox2 KO mice into WT animals did not reduce IR-induced lung injury, indicating that endothelial, but not leukocyte, NADPH oxidase–derived superoxide plays an important role in the pathogenesis of early IR injury. Several studies indicate that endothelial NADPH oxidase may contribute to ROS production during IR. Stimuli relevant to IR that can activate endothelial NADPH oxidase include 1) hypoxia-reoxygenation,[148] 2) membrane depolarization,[149] 3) flow cessation,[150] and 4) nutrient deprivation.[151] Pulmonary endothelial-derived ROS production from this enzyme complex could explain the presence of a PMN leukocyte-independent component of lung ischemia/reperfusion injury.[136]

Heumüller et al. [100] recently questioned the ability of apocynin to inhibit an NADPH oxidase in endothelial cells. To be effective apocynin has to be converted to an active dimer by myeloperoxidase. Heumüller et al.[100] reported that the inhibitory action of apocynin for NADPH oxidase is restricted to myeloperoxidase-expressing cells. According to the authors, in non-phagocytic cells the compound does not inhibit NADPH oxidase but, rather, operates as an ROS scavenger.[100] However, apocynin can form active dimers in endothelial cells through peroxidases other than myeloperoxidase [152]. Furthermore, endothelial cells can internalize myeloperoxidase released into the vessel by leukocytes.[153] These data may explain the NADPH oxidase inhibitory effects of apocynin in our study.

Interestingly, both selective reconstitution and inactivation of NADPH oxidase in leukocytes were associated with attenuated intravascular ROS release. One possible explanation is that ROS is derived from several sources, each of which produces ROS at concentrations below the ESR detection limit, which is about 10^{-9} mol/L under optimal conditions.[154] Consequently, if one (or several) source(s) of ROS is inhibited or deleted, an overall reduction in the ROS signal is measured.

In conclusion, our findings indicate that endothelial, but not leukocyte, NADPH oxidase–derived superoxide plays an important role in the pathogenesis of lung injury during the early phase of reperfusion. Therefore, selective inhibition of NADPH oxidase from endothelial cells represents a potential preventive or therapeutic strategy for the treatment of IR-induced lung injury.

7. Summary

Pulmonary ischemia/reperfusion lung injury is an important phenomenon encountered in many clinical situations, including lung transplantation and thrombolysis after pulmonary embolism. Pulmonary IR results in endothelial damage and dysfunction leading to the development of high permeability pulmonary edema. Reactive oxygen species (ROS) have been implicated in the pathogenesis of lung ischemia/reperfusion (IR) injury, although their source(s) remains unclear.

We studied the role of phagocyte-type NADPH oxidase in this process, using a model of isolated buffer-perfused mouse lungs. Ischemia was induced by stopping perfusion for 90 min. Lung injury was quantified by assessment of lung vascular permeability and fluid accumulation during reperfusion. Production of ROS was measured during reperfusion in perfusate samples from venous outflow by electron spin resonance spectroscopy using the spin probe 1-hydroxy-3-carboxy-2,2,5,5-tetramethylpyrrolidine. The relative contribution of NADPH oxidase expressed on resident leukocytes versus NADPH oxidase on endothelial cells was further studied in bone-marrow (BM)-transplanted chimeras.

In wild-type mouse lungs, IR resulted in increased vascular permeability and edema formation that was associated with increased intravascular ROS release. Pretreatment with superoxide dismutase or apocynin, an NADPH oxidase inhibitor, significantly attenuated lung injury and ROS generation. Nox2 is the catalytic subunit of phagocyte-type NADPH oxidase. Decreased tissue injury in lungs from Nox2 knockout mice was associated with reduced ROS production.

The relative contribution of NADPH oxidase expressed by resident leukocytes versus endothelial cells was further studied in bone marrow-transplanted chimeras. When NADPH oxidase in resident leukocytes was selectively inactivated by transplanting bone marrow cells from Nox2 knockout mice into wild-type animals, IR-induced tissue injury was comparable to that in wild-type mouse lungs. Conversely, transplanting bone marrow cells from wild-type mice into Nox2 knockout animals selectively reconstituted NADPH oxidase from resident leukocytes and offered protection against IR-induced lung injury.

Collectively, these findings suggest that endothelial NADPH oxidase contributes to lung injury in early reperfusion, but leukocyte NADPH oxidase does not.

8. Zusammenfassung

Das pulmonale Ischämie-Reperfusions(IR)-Syndrom ist gekennzeichnet durch eine schwere Beeinträchtigung der Ventilations-/Perfusionsverteilung (Matching), in der Folge einer endothelialen Dysfunktion mit erhöhter mikrovaskulärer Permeabilität. Diese Organschädigung kann klinisch bis hin zur Entwicklung eines kompletten Lungenversagens führen. Diese Form des akuten Organversagens hat eine große klinische Relevanz nach Lungentransplantationen sowie bei der operativen oder fibrinolytischen Desobliteration von Lungengefäßen nach akuten oder chronisch rezidivierenden Embolien. Reaktiven Sauerstoffspezies (ROS) wird eine zentrale Bedeutung für die Pathogenese von IR-Schäden beigemessen. Auch bei Ischämie und Reperfusion der pulmonalen Zirkulation wurde eine Generierung von ROS nachgewiesen. Trotz zunehmender Erkenntnisse über die Mechanismen zur Entstehung des I/R-Syndroms wurde die potenzielle Quelle reaktiver Sauerstoffspezies noch nicht eindeutig identifiziert.

Die im Rahmen dieser Arbeit durchgeführten Untersuchungen erfolgten in isoliert perfundierten und ventilierten Lungen von Wildtyp und Nox2-defizienten Mäusen. Die Mauslungen wurden Ischämiezeiten von 1,5 Stunden ausgesetzt. Post-ischämische Perfusionsstörungen wurden mit Hilfe der Quantifizierung der endothelialen Permeabilität durch Messung des kapillären Filtrationskoeffizienten und Nettoflüssigkeitseinlagerung evaluiert. Die ROS-Produktion wurde im intakten Organ mit Elektronenspinresonanz-Spektroskopie (ESR) durch Verwendung des Spin-traps 1-hydroxy-3-carboxy-pyrrolidine gemessen und in separaten Experimenten durch Zugabe von Superoxiddismutase (SOD) quantifiziert. Zudem wurden durch Knochenmarkstransplantation chimäre Mäuse generiert, um die Differenzierung des relativen Anteils der granulozytären versus der endothelialen Nox2 am IR-Schaden aufzeigen zu können.

In Lungen von Wildtyp-Mäusen wurde eine signifikante Superoxid-Freisetzung im Anschluss an die Reperfusion nachgewiesen, weiterhin kam es zur Ausbildung eines Lungenödems als Zeichen eines Lungenschadens. Die Applikation von SOD und NADPH-Oxidase-Inhibitor Apocynin zu Beginn der Ischämiephase inhibierte die erhöhte Permeabilität und Ödembildung bei der Reperfusion. So konnten wir feststellen, dass die

Lungen von Nox2-defizienten vor einem Reperfusionsschaden geschützt waren. Weiterhin konnte eine geringere Superoxid-Freisetzung in Lungen von Nox2-defizienten Mäusen nachgewiesen werden.

Die selektive Ausschaltung der NADPH-Oxidase intrapulmonaler Leukozyten durch Knochenmarkstransplantation von Nox2-defizienten Mäusen in Wildtypmäuse, zeigte keine ödemprotektive Wirkung. Im Gegensatz hierzu, ließ sich die mikrovaskuläre Schrankenstörung reduzieren, wenn Knochenmark von Wildtypmäusen in Nox2-defiziente Mäuse transplantiert wurde. Erstaunlicherweise konnte eine geringe intravaskuläre ROS-Freisetzung in den Lungen beider chimärer Mäusestämme gezeigt werden.

In Anbetracht der gezeigten Ergebnisse konnten wir der endothelialen NADPH-Oxidase die Hauptrolle in der Vermittlung des IR-Schadens der Lunge zuordnen, wohingegen überraschenderweise die leukozytäre NADPH-Oxidase nur eine nach geordneter Rolle zu spielen scheint.

References

1. Parks DA, Shah AK, Granger DN. Oxygen radicals: effects on intestinal vascular permeability. *Am J Physiol.* 1984;247:G167-170.

2. Christie JD, Kotloff RM, Pochettino A, Arcasoy SM, Rosengard BR, Landis JR, Kimmel SE. Clinical risk factors for primary graft failure following lung transplantation. *Chest.* 2003;124:1232-1241.

3. Sleiman C, Mal H, Fournier M, Duchatelle JP, Icard P, Groussard O, Jebrak G, Mollo JL, Raffy O, Roue C, et al. Pulmonary reimplantation response in single-lung transplantation. *Eur Respir J.* 1995;8:5-9.

4. Christie JD, Bavaria JE, Palevsky HI, Litzky L, Blumenthal NP, Kaiser LR, Kotloff RM. Primary graft failure following lung transplantation. *Chest.* 1998;114:51-60.

5. de Perrot M, Liu M, Waddell TK, Keshavjee S. Ischemia-reperfusion-induced lung injury. *Am J Respir Crit Care Med.* 2003;167:490-511.

6. Fiser SM, Tribble CG, Long SM, Kaza AK, Kern JA, Jones DR, Robbins MK, Kron IL. Ischemia-reperfusion injury after lung transplantation increases risk of late bronchiolitis obliterans syndrome. *Ann Thorac Surg.* 2002;73:1041-1047; discussion 1047-1048.

7. Ward BJ, Pearse DB. Reperfusion pulmonary edema after thrombolytic therapy of massive pulmonary embolism. *Am Rev Respir Dis.* 1988;138:1308-1311.

8. Levinson RM, Shure D, Moser KM. Reperfusion pulmonary edema after pulmonary artery thromboendarterectomy. *Am Rev Respir Dis.* 1986;134:1241-1245.

9. Miller WT, Jr., Osiason AW, Langlotz CP, Palevsky HI. Reperfusion edema after thromboendarterectomy: radiographic patterns of disease. *J Thorac Imaging.* 1998;13:178-183.

10. Buja LM. Myocardial ischemia and reperfusion injury. *Cardiovasc Pathol.* 2005;14:170-175.

11. Murphy GJ, Angelini GD. Side effects of cardiopulmonary bypass: what is the reality? *J Card Surg.* 2004;19:481-488.

12. Carvalho EM, Gabriel EA, Salerno TA. Pulmonary protection during cardiac surgery: systematic literature review. *Asian Cardiovasc Thorac Ann.* 2008;16:503-507.

13. Adrie C, Laurent I, Monchi M, Cariou A, Dhainaou JF, Spaulding C. Postresuscitation disease after cardiac arrest: a sepsis-like syndrome? *Curr Opin Crit Care.* 2004;10:208-212.

14. Saeed SA, Shad KF, Saleem T, Javed F, Khan MU. Some new prospects in the understanding of the molecular basis of the pathogenesis of stroke. *Exp Brain Res.* 2007;182:1-10.

15. Parks DA, Grogaard B, Granger DN. Comparison of partial and complete arterial occlusion models for studying intestinal ischemia. *Surgery.* 1982;92:896-901.

16. Braunwald E, Kloner RA. Myocardial reperfusion: a double-edged sword? *J Clin Invest.* 1985;76:1713-1719.

17. Yung G. Lung transplantation and pulmonary hypertension. *Semin Cardiothorac Vasc Anesth.* 2007;11:149-156.

18. Kennedy TP, Rao NV, Hopkins C, Pennington L, Tolley E, Hoidal JR. Role of reactive oxygen species in reperfusion injury of the rabbit lung. *J Clin Invest.* 1989;83:1326-1335.

19. Ljungman AG, Grum CM, Deeb GM, Bolling SF, Morganroth ML. Inhibition of cyclooxygenase metabolite production attenuates ischemia-reperfusion lung injury. *Am Rev Respir Dis.* 1991;143:610-617.

20. Zamora CA, Baron D, Heffner JE. Washed human platelets prevent ischemia-reperfusion edema in isolated rabbit lungs. *J Appl Physiol.* 1991;70:1075-1084.

21. Pillai R, Bando K, Schueler S, Zebly M, Reitz BA, Baumgartner WA. Leukocyte depletion results in excellent heart-lung function after 12 hours of storage. *Ann Thorac Surg.* 1990;50:211-214.

22. Minamiya Y, Tozawa K, Kitamura M, Saito S, Ogawa J. Platelet-activating factor mediates intercellular adhesion molecule-1-dependent radical production in the nonhypoxic ischemia rat lung. *Am J Respir Cell Mol Biol.* 1998;19:150-157.

23. Moore TM, Khimenko P, Adkins WK, Miyasaka M, Taylor AE. Adhesion molecules contribute to ischemia and reperfusion-induced injury in the isolated rat lung. *J Appl Physiol.* 1995;78:2245-2252.

24. Horgan MJ, Wright SD, Malik AB. Antibody against leukocyte integrin (CD18) prevents reperfusion-induced lung vascular injury. *Am J Physiol.* 1990;259:L315-319.

25. Horgan MJ, Ge M, Gu J, Rothlein R, Malik AB. Role of ICAM-1 in neutrophil-mediated lung vascular injury after occlusion and reperfusion. *Am J Physiol.* 1991;261:H1578-1584.

26. Weiss SJ. Tissue destruction by neutrophils. *N Engl J Med.* 1989;320:365-376.

27. Moraes TJ, Zurawska JH, Downey GP. Neutrophil granule contents in the pathogenesis of lung injury. *Curr Opin Hematol.* 2006;13:21-27.

28. Deeb GM, Grum CM, Lynch MJ, Guynn TP, Gallagher KP, Ljungman AG, Bolling SF, Morganroth ML. Neutrophils are not necessary for induction of ischemia-reperfusion lung injury. *J Appl Physiol.* 1990;68:374-381.

29. Steimle CN, Guynn TP, Morganroth ML, Bolling SF, Carr K, Deeb GM. Neutrophils are not necessary for ischemia-reperfusion lung injury. *Ann Thorac Surg.* 1992;53:64-72; discussion 72-63.

30. Eppinger MJ, Jones ML, Deeb GM, Bolling SF, Ward PA. Pattern of injury and the role of neutrophils in reperfusion injury of rat lung. *J Surg Res.* 1995;58:713-718.

31. Brain JD. Lung macrophages: how many kinds are there? What do they do? *Am Rev Respir Dis.* 1988;137:507-509.

32. Lehnert BE, Valdez YE, Holland LM. Pulmonary macrophages: alveolar and interstitial populations. *Exp Lung Res.* 1985;9:177-190.

33. Laskin DL, Pendino KJ. Macrophages and inflammatory mediators in tissue injury. *Annu Rev Pharmacol Toxicol.* 1995;35:655-677.

34. Bowden DH. The alveolar macrophage. *Environ Health Perspect.* 1984;55:327-341.

35. Fiser SM, Tribble CG, Long SM, Kaza AK, Kern JA, Kron IL. Pulmonary macrophages are involved in reperfusion injury after lung transplantation. *Ann Thorac Surg.* 2001;71:1134-1138; discussion 1138-1139.

36. Fiser SM, Tribble CG, Long SM, Kaza AK, Cope JT, Laubach VE, Kern JA, Kron IL. Lung transplant reperfusion injury involves pulmonary macrophages and circulating leukocytes in a biphasic response. *J Thorac Cardiovasc Surg.* 2001;121:1069-1075.

37. Naidu BV, Woolley SM, Farivar AS, Thomas R, Fraga CH, Goss CH, Mulligan MS. Early tumor necrosis factor-alpha release from the pulmonary macrophage in lung ischemia-reperfusion injury. *J Thorac Cardiovasc Surg.* 2004;127:1502-1508.

38. Zhao M, Fernandez LG, Doctor A, Sharma AK, Zarbock A, Tribble CG, Kron IL, Laubach VE. Alveolar macrophage activation is a key initiation signal for acute lung ischemia-reperfusion injury. *Am J Physiol Lung Cell Mol Physiol.* 2006;291:L1018-1026.

39. Naidu BV, Krishnadasan B, Farivar AS, Woolley SM, Thomas R, Van Rooijen N, Verrier ED, Mulligan MS. Early activation of the alveolar macrophage is critical to the development of lung ischemia-reperfusion injury. *J Thorac Cardiovasc Surg.* 2003;126:200-207.

40. Nakamura T, Abu-Dahab R, Menger MD, Schafer U, Vollmar B, Wada H, Lehr CM, Schafers HJ. Depletion of alveolar macrophages by clodronate-liposomes aggravates ischemia-reperfusion injury of the lung. *J Heart Lung Transplant.* 2005;24:38-45.

41. Kaiser L, Sparks HV, Jr. Endothelial cells. Not just a cellophane wrapper. *Arch Intern Med.* 1987;147:569-573.

42. Shah AM. Paracrine modulation of heart cell function by endothelial cells. *Cardiovasc Res.* 1996;31:847-867.

43. Ray R, Shah AM. NADPH oxidase and endothelial cell function. *Clin Sci (Lond).* 2005;109:217-226.

44. Li JM, Shah AM. Endothelial cell superoxide generation: regulation and relevance for cardiovascular pathophysiology. *Am J Physiol Regul Integr Comp Physiol.* 2004;287:R1014-1030.

45. Parker JC, Townsley MI. Evaluation of lung injury in rats and mice. *Am J Physiol Lung Cell Mol Physiol.* 2004;286:L231-246.

46. Seeger W, Walmrath D, Grimminger F, Rosseau S, Schutte H, Kramer HJ, Ermert L, Kiss L. Adult respiratory distress syndrome: model systems using isolated perfused rabbit lungs. *Methods Enzymol.* 1994;233:549-584.

47. Parker JC, Gillespie MN, Taylor AE, Martin SL. Capillary filtration coefficient, vascular resistance, and compliance in isolated mouse lungs. *J Appl Physiol.* 1999;87:1421-1427.

48. Parker JC, Prasad R, Allison RA, Wojchiechowski WV, Martin SL. Capillary filtration coefficients using laser densitometry and gravimetry in isolated dog lungs. *J Appl Physiol.* 1993;74:1981-1987.

49. Seeger W, Walmrath D, Menger M, Neuhof H. Increased lung vascular permeability after arachidonic acid and hydrostatic challenge. *J Appl Physiol.* 1986;61:1781-1789.

50. Lunde PK, Waaler BA. Transvascular fluid balance in the lung. *J Physiol.* 1969;205:1-18.

51. Taylor AE, Gaar KA. Calculation of equivalent pore radi of the pulmonary capillary and alveolar membrances. *Rev Argent Angiol.* 1969;111:25-40.

52. Hancock BJ, Landolfo KP, Hoppensack M, Oppenheimer L. Slow phase of transvascular fluid flux reviewed. *J Appl Physiol.* 1990;69:456-464.

53. Parker JC, Townsley MI. Physiological determinants of the pulmonary filtration coefficient. *Am J Physiol Lung Cell Mol Physiol.* 2008;295:L235-237.

54. Touyz RM. Reactive oxygen species, vascular oxidative stress, and redox signaling in hypertension: what is the clinical significance? *Hypertension.* 2004;44:248-252.

55. Griendling KK, Sorescu D, Ushio-Fukai M. NAD(P)H oxidase: role in cardiovascular biology and disease. *Circ Res.* 2000;86:494-501.

56. Landmesser U, Harrison DG. Oxidative stress and vascular damage in hypertension. *Coron Artery Dis.* 2001;12:455-461.

57. Zalba G, San Jose G, Moreno MU, Fortuno MA, Fortuno A, Beaumont FJ, Diez J. Oxidative stress in arterial hypertension: role of NAD(P)H oxidase. *Hypertension.* 2001;38:1395-1399.

58. Cave AC, Brewer AC, Narayanapanicker A, Ray R, Grieve DJ, Walker S, Shah AM. NADPH oxidases in cardiovascular health and disease. *Antioxid Redox Signal.* 2006;8:691-728.

59. McCord JM. Oxygen-derived free radicals in postischemic tissue injury. *N Engl J Med.* 1985;312:159-163.

60. Parks DA, Bulkley GB, Granger DN, Hamilton SR, McCord JM. Ischemic injury in the cat small intestine: role of superoxide radicals. *Gastroenterology.* 1982;82:9-15.

61. Inci I, Zhai W, Arni S, Hillinger S, Vogt P, Weder W. N-acetylcysteine attenuates lung ischemia-reperfusion injury after lung transplantation. *The Annals of Thoracic Surgery.* 2007;84:240.

62. Shargall Y, Guenther G, Ahya VN, Ardehali A, Singhal A, Keshavjee S. Report of the ISHLT working group on primary lung graft dysfunction Part VI: Treatment. *The Journal of Heart and Lung Transplantation.* 2005;24:1489.

63. Griendling KK, FitzGerald GA. Oxidative stress and cardiovascular injury: Part II: Animal and human studies. *Circulation.* 2003;108:2034-2040.

64. Jialal I, Devaraj S. Antioxidants and atherosclerosis: Don't throw out the baby with the bath water. *Circulation.* 2003;107:926-928.

65. Fridovich I. Superoxide anion radical (O2-.), superoxide dismutases, and related matters. *J Biol Chem.* 1997;272:18515-18517.

66. Schafer FQ, Buettner GR. Redox environment of the cell as viewed through the redox state of the glutathione disulfide/glutathione couple. *Free Radic Biol Med.* 2001;30:1191-1212.

67. Darley-Usmar V, Wiseman H, Halliwell B. Nitric oxide and oxygen radicals: a question of balance. *FEBS Lett.* 1995;369:131-135.

68. Al-Mehdi AB, Zhao G, Dodia C, Tozawa K, Costa K, Muzykantov V, Ross C, Blecha F, Dinauer M, Fisher AB. Endothelial NADPH oxidase as the source of oxidants in lungs exposed to ischemia or high K+. *Circ Res.* 1998;83:730-737.

69. Cremer J, Jurmann M, Dammenhayn L, Wahlers T, Haverich A, Borst HG. Oxygen free radical scavengers to prevent pulmonary reperfusion injury after heart-lung transplantation. *J Heart Transplant.* 1989;8:330-336.

70. Babior BM. The leukocyte NADPH oxidase. *Isr Med Assoc J.* 2002;4:1023-1024.

71. Taniyama Y, Griendling KK. Reactive oxygen species in the vasculature: molecular and cellular mechanisms. *Hypertension.* 2003;42:1075-1081.

72. Fantone JC, Ward PA. Polymorphonuclear leukocyte-mediated cell and tissue injury: oxygen metabolites and their relations to human disease. *Hum Pathol.* 1985;16:973-978.

73. Channon KM, Guzik TJ. Mechanisms of superoxide production in human blood vessels: relationship to endothelial dysfunction, clinical and genetic risk factors. *J Physiol Pharmacol.* 2002;53:515-524.

74. Sorescu D, Weiss D, Lassegue B, Clempus RE, Szocs K, Sorescu GP, Valppu L, Quinn MT, Lambeth JD, Vega JD, Taylor WR, Griendling KK. Superoxide production and expression of nox family proteins in human atherosclerosis. *Circulation.* 2002;105:1429-1435.

75. Jones SA, O'Donnell VB, Wood JD, Broughton JP, Hughes EJ, Jones OT. Expression of phagocyte NADPH oxidase components in human endothelial cells. *Am J Physiol.* 1996;271:H1626-1634.

76. Lassegue B, Clempus RE. Vascular NAD(P)H oxidases: specific features, expression, and regulation. *Am J Physiol Regul Integr Comp Physiol.* 2003;285:R277-297.

77. Bendall JK, Rinze R, Adlam D, Tatham AL, de Bono J, Wilson N, Volpi E, Channon KM. Endothelial Nox2 overexpression potentiates vascular oxidative stress and hemodynamic response to angiotensin II: studies in endothelial-targeted Nox2 transgenic mice. *Circ Res.* 2007;100:1016-1025.

78. Bedard K, Krause KH. The NOX family of ROS-generating NADPH oxidases: physiology and pathophysiology. *Physiol Rev.* 2007;87:245-313.

79. Lambeth JD. NOX enzymes and the biology of reactive oxygen. *Nat Rev Immunol.* 2004;4:181-189.

80. Li JM, Mullen AM, Yun S, Wientjes F, Brouns GY, Thrasher AJ, Shah AM. Essential role of the NADPH oxidase subunit p47(phox) in endothelial cell superoxide production in response to phorbol ester and tumor necrosis factor-alpha. *Circ Res.* 2002;90:143-150.

81. Li JM, Shah AM. Mechanism of endothelial cell NADPH oxidase activation by angiotensin II. Role of the p47phox subunit. *J Biol Chem.* 2003;278:12094-12100.

82. Cross AR, Jones OT. The effect of the inhibitor diphenylene iodonium on the superoxide-generating system of neutrophils. Specific labelling of a component polypeptide of the oxidase. *Biochem J.* 1986;237:111-116.

83. Cross AR, Jones OT. Enzymic mechanisms of superoxide production. *Biochim Biophys Acta.* 1991;1057:281-298.

84. O'Donnell BV, Tew DG, Jones OT, England PJ. Studies on the inhibitory mechanism of iodonium compounds with special reference to neutrophil NADPH oxidase. *Biochem J.* 1993;290 (Pt 1):41-49.

85. Stuehr DJ, Fasehun OA, Kwon NS, Gross SS, Gonzalez JA, Levi R, Nathan CF. Inhibition of macrophage and endothelial cell nitric oxide synthase by diphenyleneiodonium and its analogs. *Faseb J.* 1991;5:98-103.

86. Doussiere J, Vignais PV. Diphenylene iodonium as an inhibitor of the NADPH oxidase complex of bovine neutrophils. Factors controlling the inhibitory potency of diphenylene iodonium in a cell-free system of oxidase activation. *Eur J Biochem.* 1992;208:61-71.

87. Li Y, Trush MA. Diphenyleneiodonium, an NAD(P)H oxidase inhibitor, also potently inhibits mitochondrial reactive oxygen species production. *Biochem Biophys Res Commun.* 1998;253:295-299.

88. Cai H, Griendling KK, Harrison DG. The vascular NAD(P)H oxidases as therapeutic targets in cardiovascular diseases. *Trends Pharmacol Sci.* 2003;24:471-478.

89. Diatchuk V, Lotan O, Koshkin V, Wikstroem P, Pick E. Inhibition of NADPH oxidase activation by 4-(2-aminoethyl)-benzenesulfonyl fluoride and related compounds. *J Biol Chem.* 1997;272:13292-13301.

90. Cifuentes ME, Pagano PJ. Targeting reactive oxygen species in hypertension. *Curr Opin Nephrol Hypertens.* 2006;15:179-186.

91. Lambeth JD, Krause KH, Clark RA. NOX enzymes as novel targets for drug development. *Semin Immunopathol.* 2008;30:339-363.

92. Rey FE, Cifuentes ME, Kiarash A, Quinn MT, Pagano PJ. Novel competitive inhibitor of NAD(P)H oxidase assembly attenuates vascular O(2)(-) and systolic blood pressure in mice. *Circ Res.* 2001;89:408-414.

93. Shi J, Ross CR, Leto TL, Blecha F. PR-39, a proline-rich antibacterial peptide that inhibits phagocyte NADPH oxidase activity by binding to Src homology 3 domains of p47 phox. *Proc Natl Acad Sci U S A.* 1996;93:6014-6018.

94. Korthuis RJ, Gute DC, Blecha F, Ross CR. PR-39, a proline/arginine-rich antimicrobial peptide, prevents postischemic microvascular dysfunction. *Am J Physiol.* 1999;277:H1007-1013.

95. Chan YR, Gallo RL. PR-39, a syndecan-inducing antimicrobial peptide, binds and affects p130(Cas). *J Biol Chem.* 1998;273:28978-28985.

96. Engels F, Renirie BF, Hart BA, Labadie RP, Nijkamp FP. Effects of apocynin, a drug isolated from the roots of Picrorhiza kurroa, on arachidonic acid metabolism. *FEBS Lett.* 1992;305:254-256.

97. Stolk J, Hiltermann TJ, Dijkman JH, Verhoeven AJ. Characteristics of the inhibition of NADPH oxidase activation in neutrophils by apocynin, a methoxy-substituted catechol. *Am J Respir Cell Mol Biol.* 1994;11:95-102.

98. Meyer JW, Holland JA, Ziegler LM, Chang MM, Beebe G, Schmitt ME. Identification of a functional leukocyte-type NADPH oxidase in human endothelial cells:a potential atherogenic source of reactive oxygen species. *Endothelium.* 1999;7:11-22.

99. Suzuki Y, Wang W, Vu TH, Raffin TA. Effect of NADPH oxidase inhibition on endothelial cell ELAM-1 mRNA expression. *Biochem Biophys Res Commun.* 1992;184:1339-1343.

100. Heumuller S, Wind S, Barbosa-Sicard E, Schmidt HH, Busse R, Schroder K, Brandes RP. Apocynin is not an inhibitor of vascular NADPH oxidases but an antioxidant. *Hypertension.* 2008;51:211-217.

101. Touyz RM. Apocynin, NADPH oxidase, and vascular cells: a complex matter. *Hypertension.* 2008;51:172-174.

102. Dikalov SI, Dikalova AE, Mason RP. Noninvasive diagnostic tool for inflammation-induced oxidative stress using electron spin resonance spectroscopy and an extracellular cyclic hydroxylamine. *Arch Biochem Biophys.* 2002;402:218-226.

103. Dikalov S, Grigor'ev IA, Voinov M, Bassenge E. Detection of superoxide radicals and peroxynitrite by 1-hydroxy-4-phosphonooxy-2,2,6,6-tetramethylpiperidine: quantification of extracellular superoxide radicals formation. *Biochem Biophys Res Commun.* 1998;248:211-215.

104. Dikalov S, Skatchkov M, Bassenge E. Spin trapping of superoxide radicals and peroxynitrite by 1-hydroxy-3-carboxy-pyrrolidine and 1-hydroxy-2,2,6, 6-tetramethyl-4-oxo-piperidine and the stability of corresponding nitroxyl radicals towards biological reductants. *Biochem Biophys Res Commun.* 1997;231:701-704.

105. Becker LB. New concepts in reactive oxygen species and cardiovascular reperfusion physiology. *Cardiovasc Res.* 2004;61:461-470.

106. Weissmann N, Akkayagil E, Quanz K, Schermuly RT, Ghofrani HA, Fink L, Hanze J, Rose F, Seeger W, Grimminger F. Basic features of hypoxic pulmonary vasoconstriction in mice. *Respir Physiol Neurobiol.* 2004;139:191-202.

107. Voswinckel R, Ziegelhoeffer T, Heil M, Kostin S, Breier G, Mehling T, Haberberger R, Clauss M, Gaumann A, Schaper W, Seeger W. Circulating vascular progenitor cells do not contribute to compensatory lung growth. *Circ Res.* 2003;93:372-379.

108. Weissmann N, Kuzkaya N, Fuchs B, Tiyerili V, Schafer RU, Schutte H, Ghofrani HA, Schermuly RT, Schudt C, Sydykov A, Egemnazarow B, Seeger W, Grimminger F. Detection of reactive oxygen species in isolated, perfused lungs by electron spin resonance spectroscopy. *Respir Res.* 2005;6:86.

109. Kuzkaya N, Weissmann N, Harrison DG, Dikalov S. Interactions of peroxynitrite with uric acid in the presence of ascorbate and thiols: implications for uncoupling endothelial nitric oxide synthase. *Biochem Pharmacol.* 2005;70:343-354.

110. Schutte H, Witzenrath M, Mayer K, Weissmann N, Schell A, Rosseau S, Seeger W, Grimminger F. The PDE inhibitor zaprinast enhances NO-mediated protection against vascular leakage in reperfused lungs. *Am J Physiol Lung Cell Mol Physiol.* 2000;279:L496-502.

111. Moore TM, Khimenko PL, Taylor AE. Endothelial damage caused by ischemia and reperfusion and different ventilatory strategies in the lung. *Chin J Physiol.* 1996;39:65-81.

112. Dodd OJ, Pearse DB. Effect of the NADPH oxidase inhibitor apocynin on ischemia-reperfusion lung injury. *Am J Physiol Heart Circ Physiol.* 2000;279:H303-312.

113. Dodd-o JM, Hristopoulos ML, Welsh-Servinsky LE, Tankersley CG, Pearse DB. Strain-specific differences in sensitivity to ischemia-reperfusion lung injury in mice. *J Appl Physiol.* 2006;100:1590-1595.

114. Gorlach A, Brandes RP, Nguyen K, Amidi M, Dehghani F, Busse R. A gp91phox containing NADPH oxidase selectively expressed in endothelial cells is a major source of oxygen radical generation in the arterial wall. *Circ Res.* 2000;87:26-32.

115. Haque MZ, Majid DS. Assessment of renal functional phenotype in mice lacking gp91PHOX subunit of NAD(P)H oxidase. *Hypertension.* 2004;43:335-340.

116. Amieux PS, Cummings DE, Motamed K, Brandon EP, Wailes LA, Le K, Idzerda RL, McKnight GS. Compensatory regulation of RIalpha protein levels in protein kinase A mutant mice. *J Biol Chem.* 1997;272:3993-3998.

117. Shiloh MU, MacMicking JD, Nicholson S, Brause JE, Potter S, Marino M, Fang F, Dinauer M, Nathan C. Phenotype of mice and macrophages deficient in both phagocyte oxidase and inducible nitric oxide synthase. *Immunity.* 1999;10:29-38.

118. Pearse DB, Becker PM. Effect of time and vascular pressure on permeability and cyclic nucleotides in ischemic lungs. *Am J Physiol Heart Circ Physiol.* 2000;279:H2077-2084.

119. Pinsky DJ, Naka Y, Chowdhury NC, Liao H, Oz MC, Michler RE, Kubaszewski E, Malinski T, Stern DM. The nitric oxide/cyclic GMP pathway in organ transplantation: critical role in successful lung preservation. *Proc Natl Acad Sci U S A.* 1994;91:12086-12090.

120. Vazquez-Torres A, Jones-Carson J, Mastroeni P, Ischiropoulos H, Fang FC. Antimicrobial actions of the NADPH phagocyte oxidase and inducible nitric oxide synthase in experimental salmonellosis. I. Effects on microbial killing by activated peritoneal macrophages in vitro. *J Exp Med.* 2000;192:227-236.

121. Cale AR, Katzmann JA, Tazelaar HD, Miller VM, McGregor CG. Activation of polymorphonuclear leukocyte oxygen radical production during acute lung rejection in dogs: inhibition by an antiadhesion molecule monoclonal antibody. *J Heart Lung Transplant.* 1993;12:948-954; discussion 955.

122. Klausner JM, Anner H, Paterson IS, Kobzik L, Valeri CR, Shepro D, Hechtman HB. Lower torso ischemia-induced lung injury is leukocyte dependent. *Ann Surg.* 1988;208:761-767.

123. Adkins WK, Taylor AE. Role of xanthine oxidase and neutrophils in ischemia-reperfusion injury in rabbit lung. *J Appl Physiol.* 1990;69:2012-2018.

124. Bishop MJ, Kowalski TF, Guidotti SM, Harlan JM. Antibody against neutrophil adhesion improves reperfusion and limits alveolar infiltrate following unilateral pulmonary artery occlusion. *J Surg Res.* 1992;52:199-204.

125. Seibert AF, Haynes J, Taylor A. Ischemia-reperfusion injury in the isolated rat lung. Role of flow and endogenous leukocytes. *Am Rev Respir Dis.* 1993;147:270-275.

126. Ermert L, Seeger W, Duncker HR. Computer-assisted morphometry of the intracapillary leukocyte pool in the rabbit lung. *Cell Tissue Res.* 1993;271:469-476.

127. Martin BA, Wiggs BR, Lee S, Hogg JC. Regional differences in neutrophil margination in dog lungs. *J Appl Physiol.* 1987;63:1253-1261.

128. Gee MH, Albertine KH. Neutrophil-endothelial cell interactions in the lung. *Annu Rev Physiol.* 1993;55:227-248.

129. Ermert L, Duncker HR, Rosseau S, Schutte H, Seeger W. Morphometric analysis of pulmonary intracapillary leukocyte pools in ex vivo-perfused rabbit lungs. *Am J Physiol.* 1994;267:L64-70.

130. Bayraktutan U, Draper N, Lang D, Shah AM. Expression of functional neutrophil-type NADPH oxidase in cultured rat coronary microvascular endothelial cells. *Cardiovasc Res.* 1998;38:256-262.

131. Bayraktutan U, Blayney L, Shah AM. Molecular characterization and localization of the NAD(P)H oxidase components gp91-phox and p22-phox in endothelial cells. *Arterioscler Thromb Vasc Biol.* 2000;20:1903-1911.

132. Yang Z, Sharma AK, Marshall M, Kron IL, Laubach VE. NADPH oxidase in bone marrow-derived cells mediates pulmonary ischemia-reperfusion injury. *Am J Respir Cell Mol Biol.* 2008.

133. Yao H, Edirisinghe I, Yang SR, Rajendrasozhan S, Kode A, Caito S, Adenuga D, Rahman I. Genetic ablation of NADPH oxidase enhances susceptibility to cigarette smoke-induced lung inflammation and emphysema in mice. *Am J Pathol.* 2008;172:1222-1237.

134. Schaper M, Leib SL, Meli DN, Brandes RP, Tauber MG, Christen S. Differential effect of p47phox and gp91phox deficiency on the course of Pneumococcal Meningitis. *Infect Immun.* 2003;71:4087-4092.

135. Millar TM, Phan V, Tibbles LA. ROS generation in endothelial hypoxia and reoxygenation stimulates MAP kinase signaling and kinase-dependent neutrophil recruitment. *Free Radic Biol Med.* 2007;42:1165-1177.

136. Lu YT, Hellewell PG, Evans TW. Ischemia-reperfusion lung injury: contribution of ischemia, neutrophils, and hydrostatic pressure. *Am J Physiol.* 1997;273:L46-54.

137. Adding LC, Bannenberg GL, Gustafsson LE. Basic experimental studies and clinical aspects of gadolinium salts and chelates. *Cardiovasc Drug Rev.* 2001;19:41-56.

138. Veldhuizen RA, Lee J, Sandler D, Hull W, Whitsett JA, Lewis J, Possmayer F, Novick RJ. Alterations in pulmonary surfactant composition and activity after experimental lung transplantation. *Am Rev Respir Dis.* 1993;148:208-215.

139. Hausen B, Rohde R, Hewitt CW, Schroeder F, Beuke M, Ramsamooj R, Schafers HJ, Borst HG. Exogenous surfactant treatment before and after sixteen hours of ischemia in experimental lung transplantation. *J Thorac Cardiovasc Surg.* 1997;113:1050-1058.

140. Erasmus ME, Petersen AH, Hofstede G, Haagsman HP, Bambang Oetomo S, Prop J. Surfactant treatment before reperfusion improves the immediate function of lung transplants in rats. *Am J Respir Crit Care Med.* 1996;153:665-670.

141. van der Kaaij NP, Haitsma JJ, Kluin J, Lambrecht BN, Lachmann B, de Bruin RW, Bogers AJ. Surfactant pretreatment ameliorates ischemia-reperfusion injury of the lung. *Eur J Cardiothorac Surg.* 2005;27:774-782.

142. van Putte BP, Cobelens PM, van der Kaaij N, Lachmann B, Kavelaars A, Heijnen CJ, Kesecioglu J. Exogenous surfactant attenuation of ischemia-reperfusion injury in the lung through alteration of inflammatory and apoptotic factors. *J Thorac Cardiovasc Surg.* 2009;137:824-828.

143. Forbes A, Pickell M, Foroughian M, Yao LJ, Lewis J, Veldhuizen R. Alveolar macrophage depletion is associated with increased surfactant pool sizes in adult rats. *J Appl Physiol.* 2007;103:637-645.

144. Baritussio A, Alberti A, Armanini D, Meloni F, Bruttomesso D. Different pathways of degradation of SP-A and saturated phosphatidylcholine by alveolar macrophages. *Am J Physiol Lung Cell Mol Physiol.* 2000;279:L91-99.

145. Kassim SY, Fu X, Liles WC, Shapiro SD, Parks WC, Heinecke JW. NADPH oxidase restrains the matrix metalloproteinase activity of macrophages. *J Biol Chem.* 2005;280:30201-30205.

146. Wang LF, Mehta S, Weicker S, Scott JA, Joseph M, Razavi HM, McCormack DG. Relative contribution of hemopoietic and pulmonary parenchymal cells to lung inducible nitric oxide synthase (iNOS) activity in murine endotoxemia. *Biochem Biophys Res Commun.* 2001;283:694-699.

147. Matute-Bello G, Lee JS, Frevert CW, Liles WC, Sutlief S, Ballman K, Wong V, Selk A, Martin TR. Optimal timing to repopulation of resident alveolar macrophages with donor cells following total body irradiation and bone marrow transplantation in mice. *J Immunol Methods.* 2004;292:25-34.

148. Sohn HY, Krotz F, Gloe T, Keller M, Theisen K, Klauss V, Pohl U. Differential regulation of xanthine and NAD(P)H oxidase by hypoxia in human umbilical vein endothelial cells. Role of nitric oxide and adenosine. *Cardiovasc Res.* 2003;58:638-646.

149. Sohn HY, Keller M, Gloe T, Morawietz H, Rueckschloss U, Pohl U. The small G-protein Rac mediates depolarization-induced superoxide formation in human endothelial cells. *J Biol Chem.* 2000;275:18745-18750.

150. Manevich Y, Al-Mehdi A, Muzykantov V, Fisher AB. Oxidative burst and NO generation as initial response to ischemia in flow-adapted endothelial cells. *Am J Physiol Heart Circ Physiol.* 2001;280:H2126-2135.

151. Wei Z, Costa K, Al-Mehdi AB, Dodia C, Muzykantov V, Fisher AB. Simulated ischemia in flow-adapted endothelial cells leads to generation of reactive oxygen species and cell signaling. *Circ Res.* 1999;85:682-689.

152. Johnson DK, Schillinger KJ, Kwait DM, Hughes CV, McNamara EJ, Ishmael F, O'Donnell RW, Chang MM, Hogg MG, Dordick JS, Santhanam L, Ziegler LM, Holland JA. Inhibition of NADPH oxidase activation in endothelial cells by ortho-methoxy-substituted catechols. *Endothelium.* 2002;9:191-203.

153. Astern JM, Pendergraft WF, 3rd, Falk RJ, Jennette JC, Schmaier AH, Mahdi F, Preston GA. Myeloperoxidase interacts with endothelial cell-surface cytokeratin 1 and modulates bradykinin production by the plasma Kallikrein-Kinin system. *Am J Pathol.* 2007;171:349-360.

154. Tarpey MM, Wink DA, Grisham MB. Methods for detection of reactive metabolites of oxygen and nitrogen: in vitro and in vivo considerations. *Am J Physiol Regul Integr Comp Physiol.* 2004;286:R431-444.

List of abbreviations

A	adenine
AEBSF	4-(2-Aminoethyl)benzenesulfonylfluoride
ATP	adenosine triphosphate
bp	base pair
C	cytosine
CO_2	carbon dioxide
CPH	1-hydroxy-3-carboxy-2,2,5,5-tetramethylpyrrolidine
DNA	deoxyribonucleic acid
dNTP	2'-deoxynucleotide-5'-triphosphate
DPI	diphenylene iodonium
DTPA	diethylenetriamine-pentaacetic acid
EDTA	ethylenediaminetetraacetic acid
ESR	electron spin resonance
G	guanine
h	hour
HAES	hydroxyethyl starch
HRB	Hepes-Ringer buffer
ICAM-1	intracellular adhesion molecule-1
IR	ischemia/reperfusion
Kfc	capillary filtration coefficient
KO	knock-out
mg	milligram
$MgCl_2$	magnesium chloride
min	minute
µg	microgram
mg	milligram
µl	microliter
ml	milliliter
µM	micromolar
N_2	nitrogen
NADPH	Nicotinamide adenine dinucleotide phosphate reduced
NaOH	Sodium hydroxide

O_2	oxygen
$O_2^{\bullet-}$	superoxide anion
PCR	polymerase chain reaction
pH	negative log of hydrogen ion concentration
Ppa	pulmonary artery pressure
ROS	reactive oxygen species
SOD	superoxide dismutase
T	thymine
TBE	Tris-Boric acid-EDTA buffer
Tris	tris (hydroxymethyl)-aminomethane
U	Units
WT	wild type

Appendix

A. Acknowledgments

I am very much thankful to Prof. Dr. Werner Seeger for giving me an opportunity to carry out this work.
My special thanks to my supervisor Prof. Dr. Ardeschir Ghofrani, who put a lot of effort and time in guiding my project. I also thank him for his valuable comments on this manuscript.
My thanks and appreciation to Prof. Ralph Schermuly and Prof. Norbert Weissmann for useful discussions and advices on this manuscript.
I would like to acknowledge Dr. Robert Voswinckel for his help in the beginning of my work and Karin Quanz for her technical assistance.
My warm thanks to Oliver Eickelberg, director of the international graduate program, MBML and to all of the MBML committee.
I sincerely thank all my colleagues and friends for their help and support during this project.
I am very much thankful to Dr. Markus Roth, Bakytbek Egemnazarov, Ahmet Bal, Nirmal Parajuli, Manish Mittal whose assistance, friendship and constant encouragement, supported me throughout this work.
Finally, I thank my family members for their patience, support and love.

This work was supported by the "Deutsche Forschungsgemeinschaft", SFB547, Project B6.

Doctoral fellowship of Akylbek Sydykov was supported by ALTANA Pharma AG

Der Lebenslauf wurde aus der elektronischen Version der Arbeit entfernt.

The curriculum vitae was removed from the electronic version of the paper.

C. Statement/Erklärung an Eides Statt

"I declare that I have completed this dissertation single-handedly without the unauthorized help of a second party and only with the assistance acknowledged therein. I have appropriately acknowledged and referenced all text passages that are derived literally from or are based on the content of published or unpublished work of others, and all information that relates to verbal communications. I have abided by the principles of good scientific conduct laid down in the charter of the Justus Liebig University of Giessen in carrying out the investigations described in the dissertation."

"Ich erkläre: Ich habe die vorgelegte Dissertation selbständig, ohne unerlaubte fremde Hilfe und nur mit den Hilfen angefertigt, die ich in der Dissertation angegeben habe. Alle Textstellen, die wörtlich oder sinngemäß aus veröffentlichten oder nicht veröffentlichten Schriften entnommen sind, und alle Angaben, die auf mündlichen Auskünften beruhen, sind als solche kenntlich gemacht. Bei den von mir durchgeführten und in der Dissertation erwähnten Untersuchungen habe ich die Grundsätze guter wissenschaftlicher Praxis, wie sie in der „Satzung der Justus-Liebig-Universität Gießen zur Sicherung guter wissenschaftlicher Praxis" niedergelegt sind, eingehalten."

Akylbek Sydykov

Giessen

27.11.2009